

LONG HAUL OPTICAL FIBER TRANSMISSION THROUGH DQPSK MODULATION



By

Shozab Shafiq

(2006-NUST-MSc PhD-Elec-09)

**College of Electrical and Mechanical Engineering
National University of Sciences and Technology, Pakistan**

2008

LONG HAUL OPTICAL FIBER TRANSMISSION THROUGH DQPSK MODULATION

By

Shozab Shafiq

(2006-NUST-MSc PhD-Elec-09)

Submitted to the Department of Electrical Engineering
In Partial Fulfillment of the requirements for the Degree of
Master of Science in Electrical Engineering



**In the name of Allah, the most
Merciful and the most
Beneficent**

Dedicated to
**My Parents, Warda, Ahdab,
Phoppo and Dadi**

ABSTRACT

In this report, a SIMULINK model has been proposed for the optically amplified DWDM optical transmission system. Given that the demands of ultra-wideband transmission over the Internet, transmission techniques are now considered to be very important. The choice of modulation format used is very important to minimize the fiber dispersion and impairments due to nonlinear effects.

Either by deployment of new advanced fibers with ultra-high bit rate or upgrading RZ- 10 Gb/s DWDM optical systems to 40 Gb/s channels, the transmission capacity can be extended to Terabit/s. Modulation formats are considered to be the most efficient technique to respond to current demands and moderately simple to implement in the photonic domain and offer 3-6 dB power gain as well as much more tolerable to linear and nonlinear dispersion impairments. This research work presents DQPSK transmission technique of single light wave channel over optical fiber communication systems. It is capable of doubling the bit-rate compared to conventional OOK (On-Off Keying) signaling techniques. Corning SMF (Single Mode Fiber)-28 has been modeled along with its impairments and dispersions.

The versatile nature of this SIMULINK model demonstrates the effects of mismatched dispersion management; hence dispersion penalty in fiber transmission links. DCF (Dispersion Compensating Fiber) model has been proposed to compensate all the impairments and to retrieve the data as it was originally sent. Photonic components integrated in the model can be user-defined, enhanced or removed as desired. Essential theoretical background of the design of the optical DQPSK system is given. Detailed operation and purpose of each component model and its representation in SIMULINK block sets are described. Stages required for future extension of this simulator to support DWDM operations to allow Tb/s transmission are also outlined.

ACKNOWLEDGMENTS

All praise to **Almighty ALLAH**, who is the Supreme authority, Lord of the word guides in darkness and helps in all difficulties. All respect to the Holy Prophet (SAW) who enabled us to recognize our creator and the golden principles of Islam. Along with Almighty ALLAH's help there are so many who have contributed to the success of this journey.

Working under the supervision of Dr. Ejaz Muhammad, my supervisor, was really a great honor for me. He remained a source of motivation for me to complete my research work in stipulated time and his valuable guidance enabled me to move in right direction without wasting time. My great regards are for my parents who prayed day and night for my success.

I am indebted to **Dr. Khalid Munawar** and **Dr. Mohammad Bilal Malik**, who permitted me to avail the facilities of Control Lab for my research work. I would also like to thank **Mr. Taosif Iqbal, Mr. Asim Ajaz and Maj. Muhammad Salman** for their interest in my project and for their valuable guidance throughout my work. They helped me a lot in solving my Software problems.

TABLE OF CONTENTS

1. Introduction	
1.1 Introduction.....	2
1.2 Background.....	2
1.3 DWDM Optical Transmission System.....	2
2. Transmitter	
2.1 Transmitter Basics	7
2.1.1 Laser Source.....	7
2.1.2 RZ- Encoding.....	8
2.1.2 External Modulator.....	8
2.1.3 Modulation Format.....	10
2.2 SIMULINK Model.....	13
2.2.1 M-file Definitions.....	14
2.2.2 Assumptions.....	14
2.2.3 Source Model.....	15
2.2.4 Sampling.....	15
2.2.5 MZIM & RZ Pulse Shaping.....	16
2.2.6 Phase Modulator Model.....	18
2.3 Simulation Results.....	19
3. Optical Fiber Channel	
3.1 Brief Introduction.....	24
3.2 Optical Fiber Impairments.....	25
3.3 Corning Single Mode Optical Fiber.....	26
3.3.1 The Standard for Performance.....	26

3.3.2	Features and Benefits.....	26
3.3.3	The Sales Leader.....	26
3.3.4	Attenuation Levels.....	26
3.3.5	Dispersion.....	27
3.4	Linear Fiber Propagation Model	28
3.4.1	Derivation of SMF Transfer Function Model....	28
3.5	SIMULINK Model.....	31
3.6	Simulation Results.....	34
4.	Receiver	
4.1	Receiver.....	35
4.2	Noise Sources.....	39
4.3	SIMULINK Model.....	40
4.3.1	MZDI Model.....	42
4.3.2	Photodiode Model.....	44
4.3.3	Photodiode/Amplifier Noise Model.....	45
4.3.4	Amplifier Model.....	46
4.4	Bit Error Rate Calculations.....	48
4.5	Simulation Results.....	49
5.	Conclusions and Recommendations	
5.1	Conclusion.....	54
5.2	Recommendations.....	54
	Appendix.....	58
	References.....	59

List of Figures

1.1	Architecture of a DWDM system.....	4
1.2	Single Mode Optical Fiber Cable.....	5
2.1	DFB Laser Diode.....	7
2.2	Mach-Zehnder Interferometer Modulator.....	9
2.3	MZIM Voltage-Power Characteristic Curve.....	10
2.4	DQPSK Waveforms.....	12
2.5	DQPSK Signal Constellations.....	12
2.6	DQPSK Optical Fiber Transmission Model.....	13
2.7	RZ-DQPSK Transmitter Model.....	14
2.8	Mach-Zehnder Interferometer Modulator Model.....	16
2.9	RZ-Pulse Shaping.....	17
2.10	DQPSK Modulator Model.....	18
2.11	Input Signal Spectrum.....	19
2.12	Transmitted Signal's Eye Diagram.....	20
2.13	PM ($\pi/2$) Electrical Bit stream.....	20
2.14	PM (π) Electrical Bit stream.....	21
2.15	Modulated Data from PM ($\pi/2$).....	21
2.16	Modulated Data from PM (π).....	22
2.17	Transmitted Data Constellation.....	22
3.1	Spectral Attenuation Graph for SMF-28	27
3.2	Linear Fiber Model, a Low Pass Filter	32
3.3	Optical Fiber Channel SIMULINK Block Model	33
3.4	Eye Pattern before Fiber Transmission	34
3.5	Pattern after Fiber Transmission (Uncompensated).....	35
3.6	Eye Pattern after Compensation (DCF)	35

4.1	Delay Interferometer.....	37
4.2	Phase to Intensity Characteristics of MZDI	38
4.3	Balanced Photodiode Detection	39
4.4	Flow Chart Showing Receiver Configuration.....	40
4.5	Non-Coherent Direct Detection Configuration	41
4.6	Balanced DQPSK Receiver Model.....	41
4.7	SIMULINK Block Diagram of DQPSK Receiver.....	42
4.8	Mach-Zehnder Delay Interferometer Model	43
4.9	Photodiode/Amplifier Noise & Amplifier Model.....	47
4.10	Uncompensated Received Data.....	49
4.11	DCF Compensated Received Data.....	50
4.12	Transmitted Signal's Eye Diagram.....	50
4.13	Received Signal's Eye Diagram (No DCF)	51
4.14	Received Signal's Eye, Dispersion= -75ps/nm.km.....	52
4.15	Received Signal's Eye, Dispersion= -65ps/nm.km.....	52
4.16	Received Signal's Eye, Dispersion= -95ps/nm.km.....	53
4.17	Experimental Result	53

List of Tables

2.1	DQPSK Modulation Phase Shifts.....	11
3.1	Attenuation Levels.....	26
4.1	MITEQ LNA Amplifier Data Sheet.....	47

INTRODUCTION

1.1 Introduction

The demand for increasing the transmission capacity of optical fiber transmission systems has prompted many researchers and companies to investigate cheaper, higher bandwidth optical fiber system alternatives. A substantial amount of research has been pursued in developing high transmission rate systems which now extend into the terabit per second region. A large proportion of these investigations have focused on the design of optical systems as a whole. Many techniques have been implemented so far to make the optical fiber transmission better such as the application of pre-transmission dispersion management, amplification and on some circumstances, using different optical carrier sources. An area of development which has had a great deal of research interest and applications is the dense wavelength division multiplexing (DWDM) optical fiber system. This system typically transmits multiple wavelengths on a single mode fiber. This method has been one of the key contributors to enhance the optical transmission channel capacity.

This report investigates the limitations of a single channel transmission driven by DQPSK signaling technique. Recently, interests have been shown towards the development of DQPSK transmission systems. These systems have been shown to be more tolerant to the effects of chromatic dispersion and other non-linear effects as compared to conventional OOK (On-Off keying) format. The DQPSK technique also doubles the spectral efficiency (b/s/Hz) by encoding two bits of data per symbol in a differential phase shift format. The development and simulation of an optical DQPSK transmission link system using MATLAB SIMULINK are described. The system is compared, to within certain limitations, with experimental results published papers. The impairments on system performance due to chromatic dispersion effects, power attenuation and receiver noise effects have been analyzed. The real performance degrading effects are included in simulations based on theoretical knowledge. The flexible nature of the simulation platform offered by SIMULINK allows simulation ease for modern optical communication systems.

1.2 Background

Before considering the details of the optical DQPSK transmitter design, the definitions, applications and theoretical background of optical components used in the model must be clear. The ITU-T standards (G.694.1) which have been recommended to ensure correct reliability and delivery of data are considered at a later stage. In this design a single channel transmission has been considered with an operating channel wavelength of 1550nm. DWDM systems typically consist of many photonic components.

1.3 DWDM Optical Transmission System

In fiber-optic communications, dense wavelength-division multiplexing (DWDM) is a technology which multiplexes multiple optical carrier signals on a single optical fiber by using different wavelengths of laser light to carry different signals. This allows for a multiplication in capacity, in addition to enabling bidirectional communications over one strand of fiber. "This is a form of frequency division multiplexing (FDM) but is commonly called wavelength division multiplexing."

Given the increase in demand for transmission capacity of modern optical fiber communication systems, considerations into alternative methods which allow for this increase need to be assessed.

There exist two alternatives;

- (1) Improve transmission bandwidth by merely increasing the data rate. Current transmitters used in some modern optical fiber systems operate at 40Gb/s. This approach can be quite costly when used in systems with several data sources (i.e. video, data etc).
- (2) Increase the number of transmitters (wavelengths) and thus the overall transmission rate by the same factor. Basically multiple wavelengths are transmitted on the one fiber. Consider for example, 20 channels operating

at 10Gb/s, each coupled in one fiber making overall transmission rate equal to 200Gb/s. With improving transmitter technology, DWDM systems have made it possible to achieve up to Terabit/sec transmission.

In this report, a single channel from the second alternative is selected as the design of choice for the optical communication system, simulating a single channel from a DWDM system operating with 10Gb/s per channel. The foundations of the DWDM system rely on the ability to couple multiple wavelengths on one transmission link. Using commercially available optical technology such as optical de/multiplexers, optical amplifiers and transmitter diodes, a point-to-point DWDM transmission system can be developed as shown below in Figure 1.1.

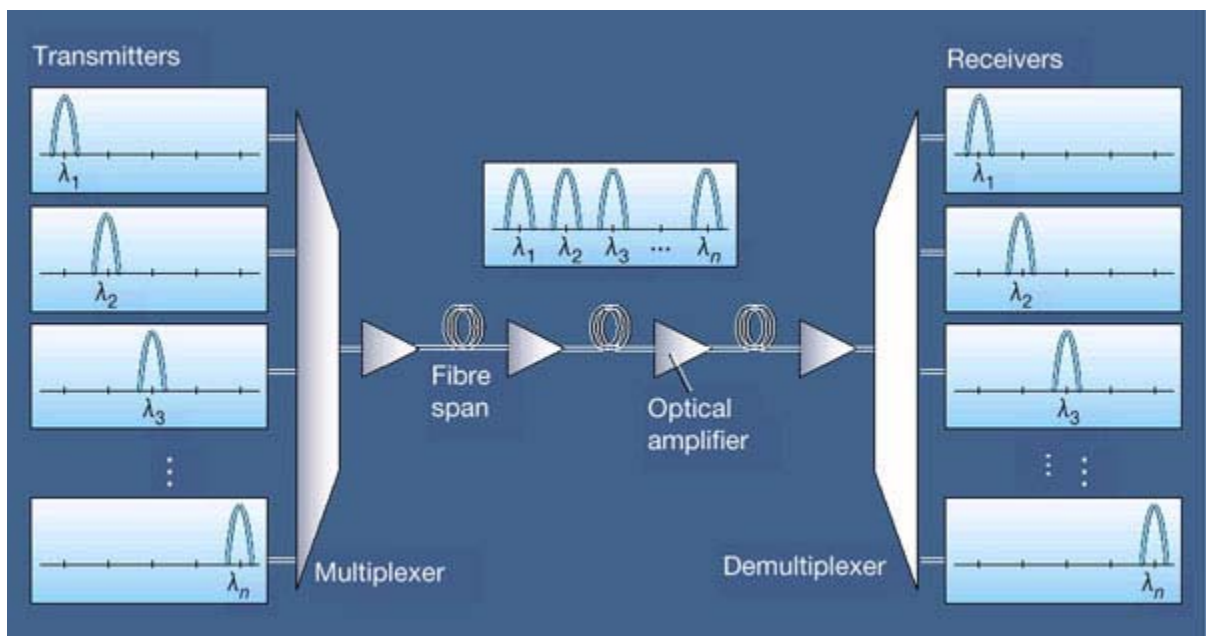


Figure 1.1 Architecture of a DWDM system

In this report project, only one Peer to Peer transmission channel link has been simulated to understand the fundamentals of DQPSK signaling technique. The simulation model consists of various optical devices with their behavior represented initially by theoretical interpretation. For example, in transmitter, the

optical components are placed in cascade which effectively modulates the optical carrier signal using a DQPSK format. The details of the transmitter configuration will be outlined later. It is important to note that the principle behind DWDM is to associate each transmitter to a different data stream or effectively a different wavelength. Optical amplifiers, dispersion compensation modules and other optical devices may be added in between fiber spans, this allows for long haul transmission to be realized. These devices typically attempt to cancel any loss or attenuation in the signal as it propagates through the fiber. The figure given below shows a typical structure of a single mode fiber.

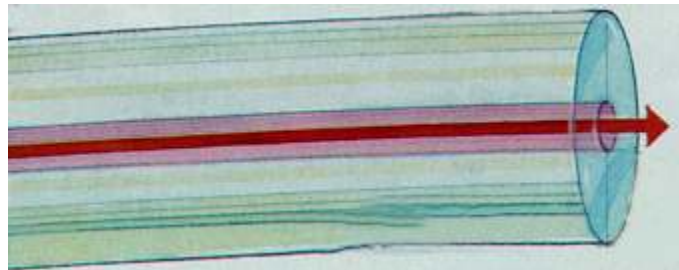


Figure 1.2 Single Mode Optical Fiber Cable

The optical receivers (Rx) normally consisting of photo detectors and other optical hardware such as a Mach-Zehnder Delay interferometer (MZDI) in case of DQPSK transmission systems and other differential encoding systems. These optical devices allow for demodulation of the received signal and allow measurements of bit error rate (BER) and other system performance parameters to be evaluated using the eye diagram monitored by the scope at an appropriate point of the system.

CHAPTER 2

TRANSMITTER

2.1 Transmitter Basics

2.1.1 Laser Source

A laser diode, like many other semiconductor devices, is formed by doping a very thin layer on the surface of a crystal wafer. The crystal is doped to produce an n-type region and a p-type region, one above the other, resulting in a $p-n$ junction, or diode.

Distributed feedback lasers (DFB) are the most common transmitter type in DWDM-systems. To stabilize the lasing wavelength, a diffraction grating is etched close to the $p-n$ junction of the diode. This grating acts like an optical filter, causing a single wavelength to be fed back to the gain region and laser. Since the grating provides the feedback that is required for lasing, reflection from the facets is not required. Thus, at least one facet of a DFB is anti-reflection coated. The DFB laser has a stable wavelength that is set during manufacturing by the pitch of the grating, and can only be tuned slightly with temperature. Such lasers are the workhorse of demanding optical communication.

Using the concept of feedback, the DFB laser diode acts as a reliable source of optical carrier in single-mode optical fiber transmission. It is constructed using a cavity enclosed at both ends by a grating. Light is reflected internally in the cavity until the phase of the incident and reflected waves are matched. The light is then allowed to propagate. In this report DFB laser diode is simulated using a signal generator.

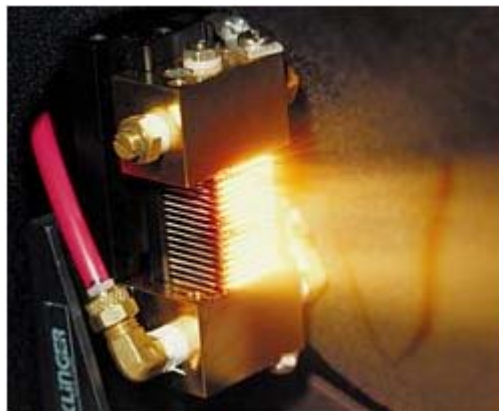


Figure 2.1 DFB Laser Diode

2.1.2 RZ Encoding

In RZ encoding, a binary 1 is represented by half period of optical pulse, present in the first half of the bit duration. Although the optical pulse is present in the first half of the bit duration, the light levels returns to 0 during the second half. Binary 0 is represented by the absence of an optical pulse during the entire bit duration. RZ encoding might require only half the bit duration for data transmission but it requires twice the bandwidth of NRZ encoding.

However, in the presence of long strings of 0s, loss of timing could arise. RZ pulses have much greater tolerance to the effects of chromatic dispersion as compared to NRZ pulses. RZ pulses maintain practical residual tolerance at much higher launch powers thus allowing inexpensive unrepeated transmission over multiple segments of fiber. This format is commonly used in metropolitan optical communications systems.

2.1.3 External Modulator

The **Mach-Zehnder interferometer** (MZIM) named after physicists Ludwig Mach is most widely used as photonic devices for external modulating the generated light waves. Although several types of MZIMs are available commercially but the one approximated in this report is lithium niobate (LiNbO_3) single electrode modulator. This modulator is well known for its use in 10Gb/s PSK systems. It is placed in cascade with DFB laser to externally modulate the carrier via the electro-optic effects.

The MZIM consists of a Y splitter (3dB), two waveguide arms and a Y combiner as shown in Figure 2.2.

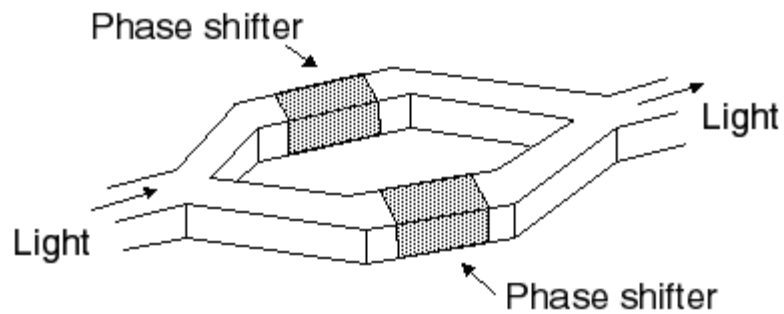


Figure 2.2 Mach-Zehnder Interferometer Modulator

The electro-optic effect allows the refractive index of the material to change as a response to an applied voltages $u_2(t)$ and $u_1(t)$. For single electrode MZIM, $u_1(t)$ equals zero. The phase of the signal which passes through this region of applied voltage (binary or sinusoidally varying) remains unchanged.

At the input, the power of the incident carrier is split equally through a “Y splitter”, one carrier wave experiences a phase change (assumed 0 or π radians in this report), while the other passes unchanged, two waves will combine at the output through “Y combiner”.

It should be noted that the optical carrier that has experienced the 0 or π phase shift (in the lower arm of MZIM) is of great importance since the differential phase of this waveform will represent the first encoded bit of the two bits (di-bit) to be transmitted. The MZIMs are biased at the minimum transmission point with biasing voltage, $V_\pi \approx 3.5v$ in practice. A typical driving “Voltage to Intensity” transfer characteristic of the MZIM is shown below.

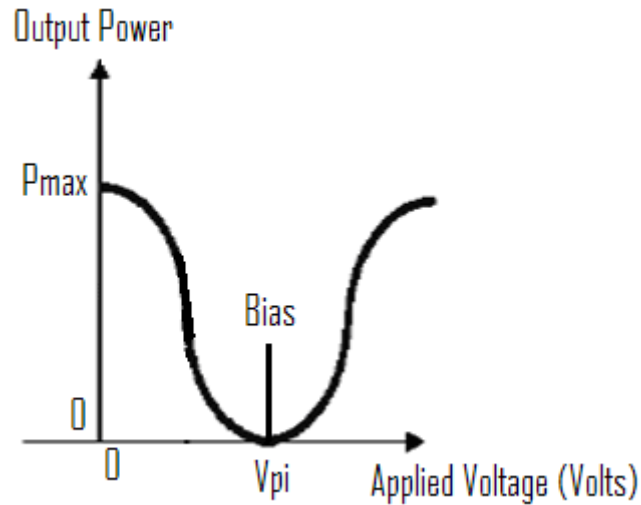


Figure 2.3 MZIM Voltage-Power Characteristic Curve

The MZIM is also a useful device in its response to certain high bit rate pulse shapes (e.g. NRZ, RZ) which can be used in place of a normal phase modulator (PM) biased to π phase shift. Other phase modulators simulated in this report operate under the same physical principles as the MZIM however are assumed to be biased to produce a phase shift of π and $\pi/2$ in the optical carrier.

2.1.4 Modulation Format

When digitizing data for transmission across many hundreds of kilometers many digital modulation formats have been proposed and investigated. This report investigates the DQPSK (Differential Quadrature Phase Shift Keying) modulation format. This modulation scheme although having been in existence for quite some time had only been implemented in the electrical domain.

Its application to optical systems proved difficult in the past as constant phase shifts of the optical carriers are to be maintained. However, with the improvement of optical technology and alternate transmitter design setup, these difficulties are eliminated.

One of the main attractive features of the DQPSK modulation format is that it offers both twice the bandwidth and increased spectral efficiency as compared to OOK. As an example, comparisons between 8 x 80Gb/s DQPSK systems and 8 x 40Gb/s OOK systems show that DQPSK modulation offers more superior performance (i.e. spectral efficiency). The very nature of the signaling process also allows non-coherent detection at a receiver to be possible, thus reducing the overall cost of the system design.

The DQPSK modulation format uses a differential form of phase shift modulation to the optical carrier which encodes the data. DQPSK is an extension to the simpler DPSK (Differential phase shift keying) format. Rather than having two possible symbol phase states (0 or π phase shift) between adjacent symbols, DQPSK is a four-symbol equivalent $\left(0, \frac{\pi}{2}, \pi, \frac{3\pi}{2}\right)$. Depending on the desired di-bit combination to be encoded, the difference in phase, $\Delta\phi_{\text{mod}}$ between the two adjacent symbols (optical carrier pulses) is varied systematically. *Table 1* outlines this behavior.

Di-Bit	Phase Difference $\Delta\phi = \phi_2 - \phi_1$ (degrees)
00	0
01	90
10	180
11	270

Table 2.1 DQPSK Modulation Phase Shifts

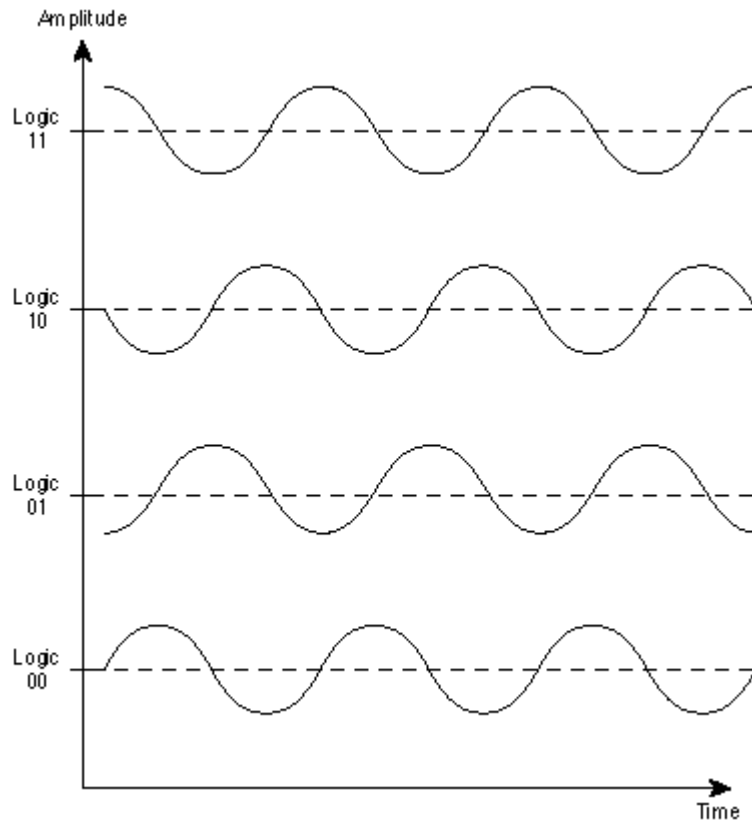


Figure 2.4 DQPSK Waveforms

The above table can also be represented in the form of a “constellation diagram”. This graphically explains the signals state in both amplitude and phase.

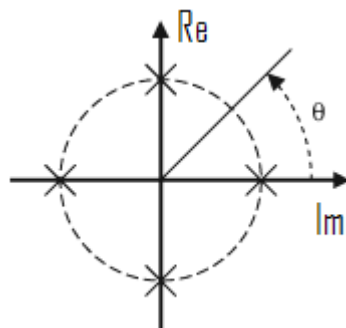


Figure 2.5 DQPSK Signal Constellations

Ideally, In DQPSK signaling, amplitude is kept constant whereas phase varies but in practice amplitude changes are also observed. These changes are due to the characteristics of MZIM which is in the form of optical intensity modulation. This is usually termed as the patterning effect. This effect is not implemented in this report due to inaccurate data pulse representation.

2.2 SIMULINK Model

In this report only a single channel is implemented using DQPSK signaling technique. The primary design of a single channel operating efficiently was considered critical.

The whole model is divided into three main stages:

- RZ-DQPSK Transmitter Model
- Single Channel Optical Fiber Model
- Balanced DQPSK Receiver Model

The block diagram showing the major components of the model is shown below.

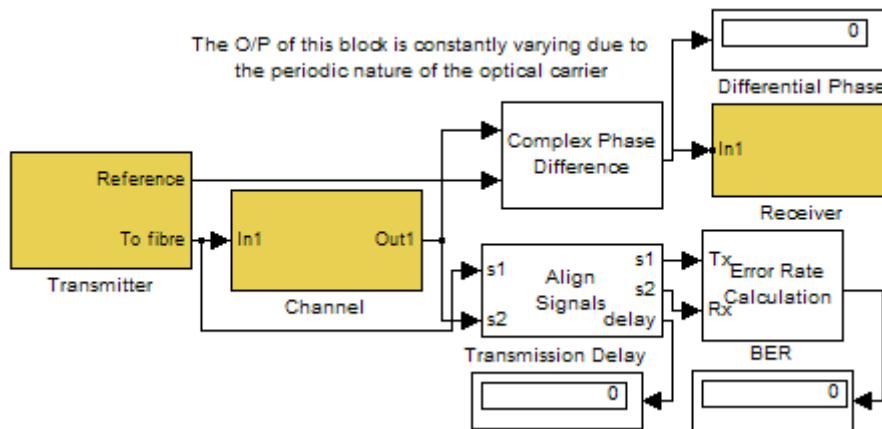


Figure 2.6 DQPSK Optical Fiber Transmission Model

The final results displayed during simulations include the *Di-bit* RZ electrical bit stream (2 x 10Gb/s) which modulates the optical carrier via phase modulator, the spectrum of the optical carrier, the RZ time-domain pulse generated, constellation diagram of the transmitted data and finally the eye diagrams both before to fiber propagation and after to allow for BER testing and other system performance measurements.

2.2.1 M-file Definitions

Variables are defined in m-file so that they can easily be changed whenever required. These variables include system parameters such as bit-rate, number of transmitted Di-Bits and fiber length. This file must be executed before simulations can begin. It also presents the opportunity to change system parameters without having to find the location of the variable in the Simulink model.

2.2.2 Assumptions

To simplify some aspects of the transmitter design, it is assumed that there are no chirping effects from DFB laser source. An ideal sine wave generator is used to represent the fixed wavelength light waves. This can be implemented using an X-cut LiNbO3 MZIM. Secondly the insertion losses (coupling losses), traveling losses or recombination losses for the MZIM are also ignored. The minimum output power ' P_{min} ' of the MZIM is modeled mathematically to be zero at the minimum transmission point. Otherwise patterning effects would be observed on the eye diagram.

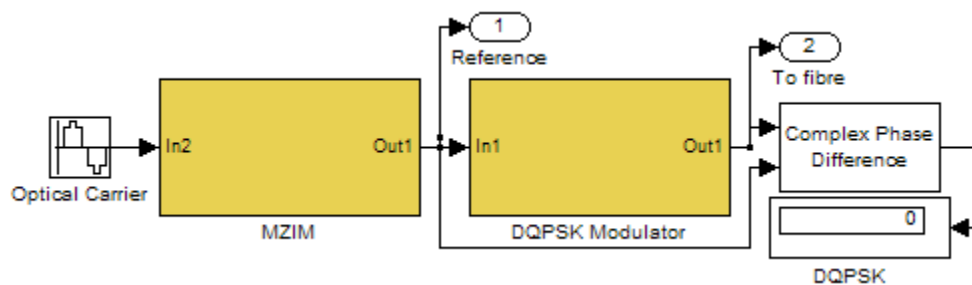


Figure 2.7 RZ-DQPSK Transmitter Model

2.2.3 Source model

As mentioned earlier, to simplify this part of the simulation development, an ideal laser source (i.e. no frequency chirp present) is implemented in Simulink by a “Sine Wave Generator” block. This block models the desired sinusoidal optical carrier obtained from an ideal DFB laser which takes the mathematical form:

$$c(t) = A \cos(\omega_n t + \phi)$$

where ω_n and ϕ are the frequency and phase of the optical carrier respectively, with $\omega = 2\pi * 1.93 * 10^{14} \text{ rad / s}$ corresponding to the 1550nm operating wavelength. A , the amplitude of the optical carrier has been normalized for simplicity and is thus set to unity.

2.2.4 Sampling

Due to the discrete nature in which Matlab stores and processes data, the waveform are sampled at Nyquist rate to ensure synchronization. Some of the blocks in Simulink have the *sample time* fields, the Nyquist sampling time is also inserted in these spaces. This technique maintains the integrity of the signals.

According to the Nyquist theorem, this sampling interval is at least twice the highest frequency in the system. Thus it comes out to be;

$$f_{\text{sampling}} \geq 2f$$
$$\therefore T_{\text{sampling}} \leq \frac{1}{2f} = 2.59 * 10^{-15} \text{ sec}$$

2.2.5 MZIM & RZ Pulse Shaping

The digital signal considered in this report is RZ (Return to Zero). This pulse shape has duration of half the period ($T/2$), thus has a 50% duty cycle. In most modern optical systems, this RZ pulse shape is often approximated by a sinusoid having frequency $\frac{1}{T}$ Hz. The brief nature of the pulse, makes the RZ pulse shape more tolerable to intersymbol interference (ISI) compared to the non-return-to-zero (NRZ) pulse shape, however its power spectra occupies a larger bandwidth.

The NRZ pulse shape also has a data rate of $\frac{1}{T}$ b/s however its duration is T seconds. The power spectrum is also reduced to half to that of the RZ pulse spectrum. RZ pulse shaping is implemented inside the MZIM block.

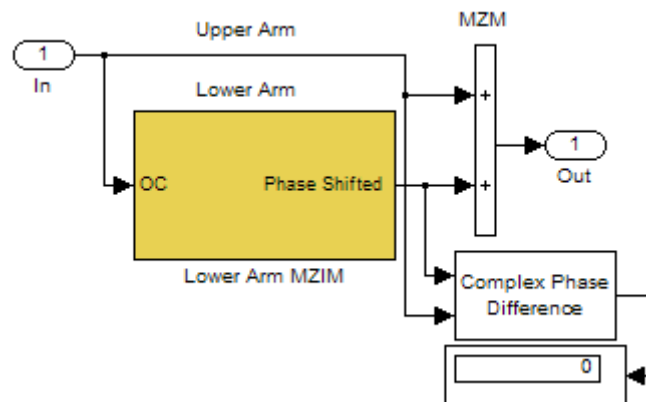


Figure 2.8 Mach-Zehnder Interferometer Modulator Model

The splitting of the optical carrier at the input of the MZIM causes the output, when viewed experimentally, to consist of two optical waveforms merging together, provided there has been some phase change in the lower arm. Thus in reality, it is the optical signal from the lower arm that is of greater importance as it has been phase shifted by $u_2(t)$.

The MZIM driving signal is constructed using a 10GHz signal of magnitude 0.5; 0.5 is added further and multiplied by π . This driving signal is modeled as;

$$u_2(t) = 0.5 + 0.5 \sin \omega t$$

The values injected to the 'Complex Phase Shift' block 'Ph' input has value between 0 and π . This block then phase shifts the optical carrier at the 'In' port by the amount of 'Ph'. The resultant signal is then added to an unaltered optical carrier simulating the Y combiner of MZIM. This signal is then passed through the DQPSK phase modulator.

Figure 2.9 shows the output of the MZIM. The result is the RZ shape of the generated light carrier.

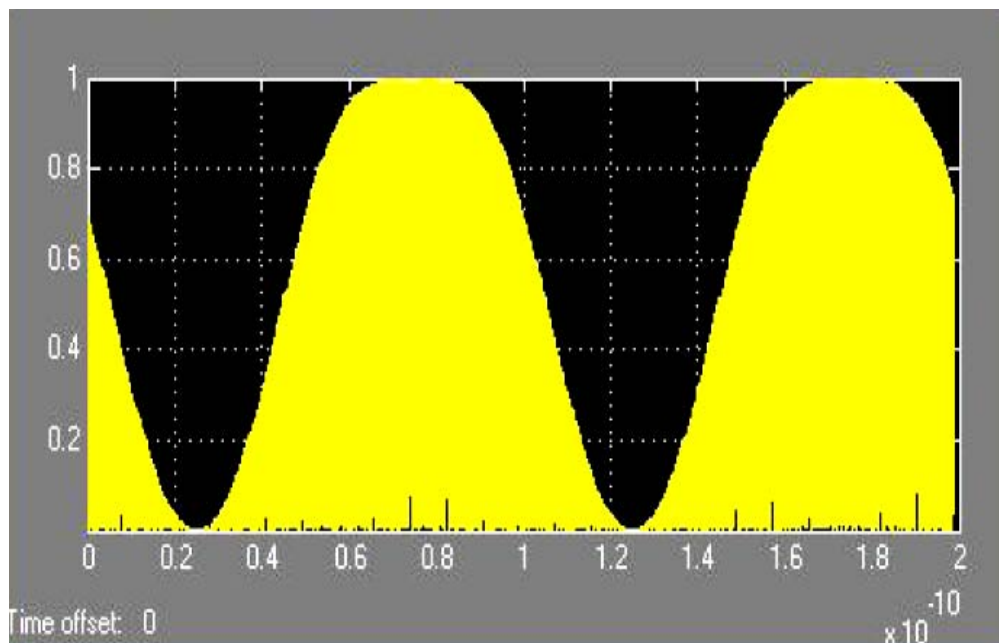


Figure 2.9 RZ-Pulse Shaping

2.2.6 Phase Modulator Model

For DQPSK transmission; two phase modulators are modeled. One induces a phase shift of 0 or π radians and the other of 0 or $\pi/2$ radians.

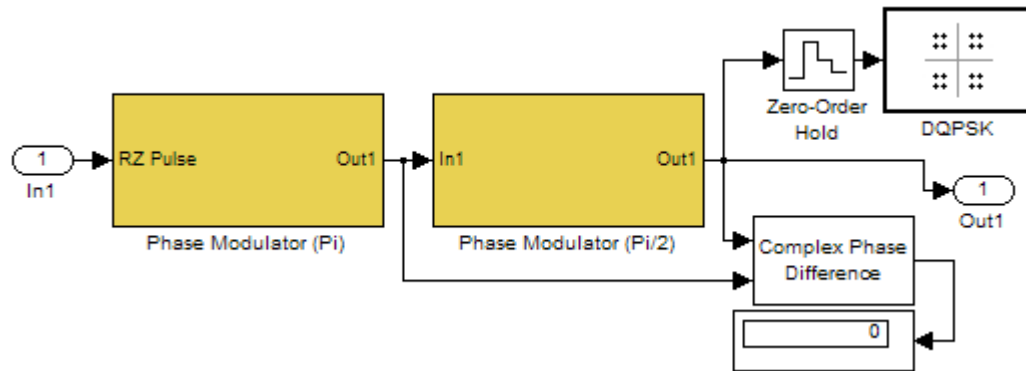


Figure 2.10 DQPSK Modulator Model

Inside the first Phase Modulator block (MZIM), the ‘Bernoulli Binary’ block generates a RZ random bit pattern which is multiplied by π in the second step to give a value ‘0’ or ‘ π ’. This value is sampled every bit period (via unit delay block every 100ps for 10Gb/s operation). Finally the RZ-pulse shaped optical carrier is phase shifted by 0 or π accordingly. “Complex Phase Shift” block of SIMULINK is used for this purpose.

The second Phase Modulator that induces a phase shift of 0 or $\pi/2$ radians in the optical carrier operates on the same principles as described above. The only difference is to multiply the random RZ bit-stream by $\pi/2$ instead of π .

The random bit streams considered in both the phase modulators are uncorrelated; this is done by inserting different “Seed” in the given space. Or it can also be done by placing an extra unit delay block after the Bernoulli Binary Generator. All the four states of the signal constellation are achieved and are observed during simulation. This would not be achieved if the two bit streams

were same. In practice the characteristic of uncorrelated data is achieved by the physical time delay due to signal propagation in between the phase modulators.

2.3 Simulation Results

In order to best analyze the developed model, scopes are placed at different points in the model. Some of the scopes are set to automatically open at the time of simulation while other can be visualized by double clicking on the scope. Figure 2.10 shows the spectrum of the input carrier signal. The spectrum clearly shows the frequency at which the signal is centered.

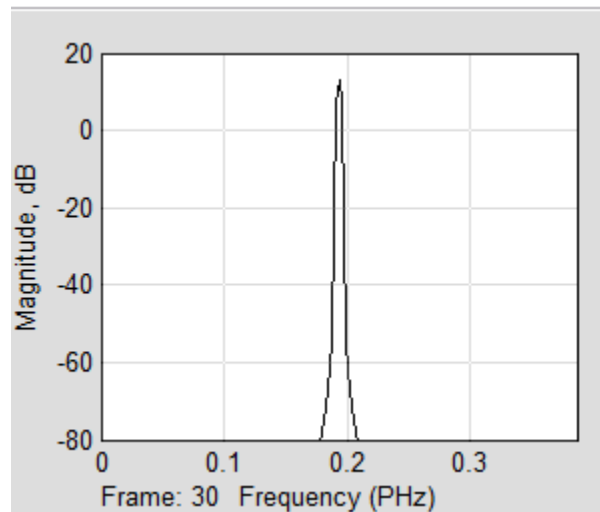


Figure 2.11 Input Signal Spectrum

Figure 2.11 shows the transmitted eye diagram. It's very obvious that the eye has maximum opening because there are no dispersion, attenuation or noise effects added. The peak amplitude of this eye is assumed to be 20. Eye diagram helps in calculating the Bit Error Rate measurements. Q-factor method has been used in this report to calculate the BER. This method is simple and easy to implement. Later on it will be shown that when the noise effects are added, a considerable amount of eye change is observed.

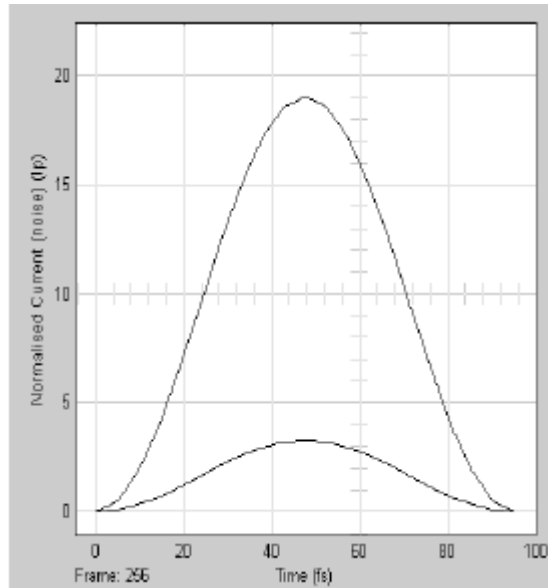


Figure 2.12 Transmitted Signal's Eye Diagram

The electrical bit streams shown in figure 2.12 and 2.13 are the inputs to the phase modulator and MZIM. Each stream has a data rate of 10Gb/s and when these two modulators are placed in cascade, the total data rate becomes $2 \times (10\text{Gb/s})$. The doubling of the data rate is because of the used modulation format that is DQPSK. Both the data streams must be uncorrelated to achieve the desired data rate.

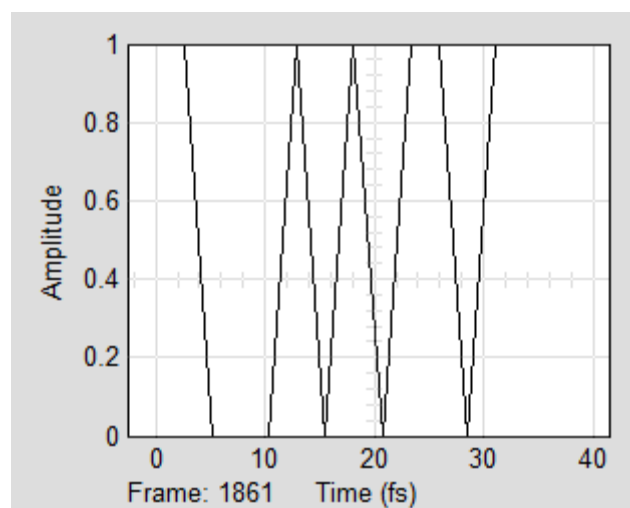


Figure 2.13 PM ($\pi/2$) Electrical Bit stream

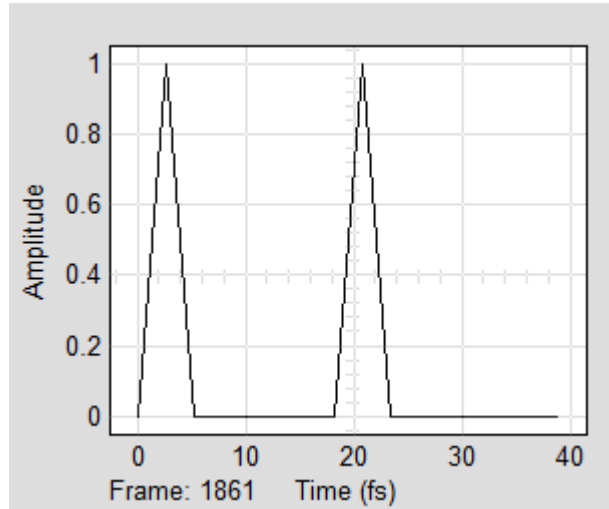


Figure 2.14 PM (π) Electrical Bit stream

Figure 2.14 and 2.15 are the output data constellations of the two phase modulators. A ' $\pi/2$ ' phase modulator which is capable of inducing phase shifts of '0' or ' $\pi/2$ ' radians whereas the Lower Arm MZIM is capable of inducing phase shifts of '0' or ' π ' radians. These two constellations represent the same.

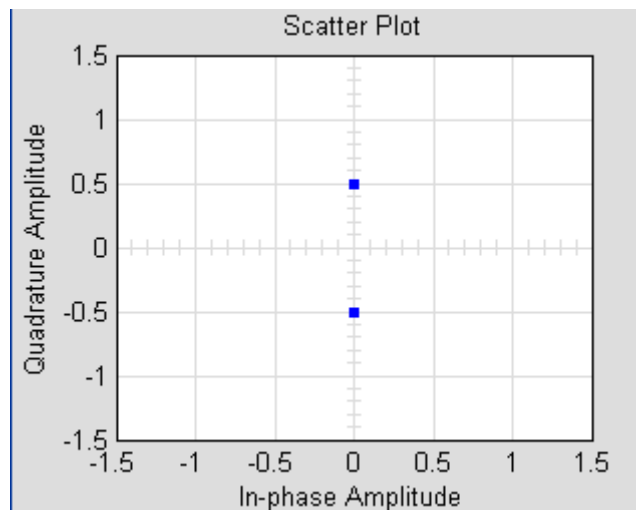


Figure 2.15 Modulated Data from PM

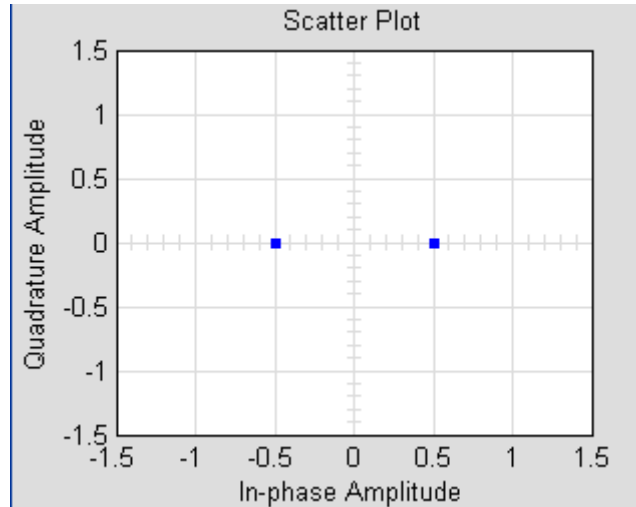


Figure 2.16 Modulated Data from MZIM

Figure 2.16 is the output of the cascaded phase modulators. The constellation diagram clearly shows that each data constellation has a phase difference of $\pi/2$ radians which will be used later on at the detection stage.

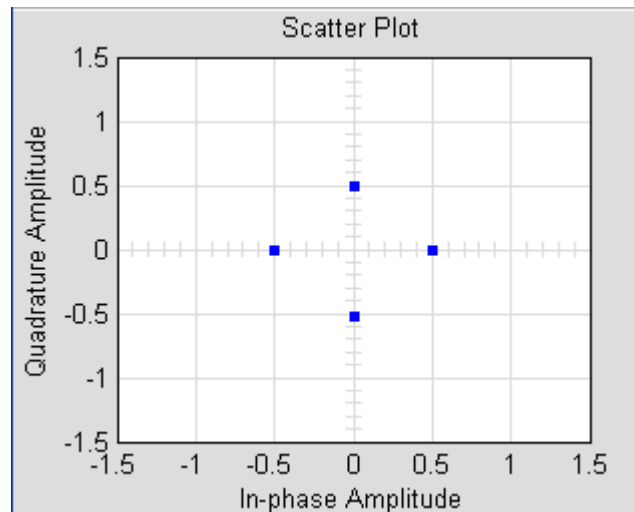


Figure 2.17 Transmitted Data Constellation

The above data constellation is the final form of the transmitted signal which is then to be transmitted via single mode optical fiber channel.

Chapter 3

OPTICAL FIBER CHANNEL



3.1 Brief Introduction

Optical communication systems and networks are installed throughout the world, from terrestrial to metropolitan to global information transport structures. The milestones include the invention of the low loss optical fibers in 70s, optical fiber amplifier in 80s and inline fiber Bragg grating in 90s. Optical communication remains a very diverse field, with ever increasing applications, e.g. long-haul communications, aircraft technology, underwater exploration, and high speed communications.

DWDM, known as Dense Wavelength Division Multiplexing is a multi-carrier fiber-optic transmission technique. Multiple-carrier optical signals are employed, digitally modulated, at bit-rate of 10Gb/s up to 40Gb/s in ultra-high speed and long haul transmission systems.

There is an ever increasing demand to upgrade the transmission capacity of multi-wavelength channels over ultra-long optical fiber distance. It includes; increased capacities, ultra-high speed, minimum transmission errors, and non-linear impairments over long distances and maximizing total number of channels over the C- L- and S- bands of the 1550 nm window.

Modeling of an optically amplified transmission system is very important. The models must be simple and accurate in representing the physical phenomena and corroborated with experimental systems. Although there are a number of modeling packages available in commercial environment such as VPI systems, OptiWave etc, they are either complicated, non user friendly or difficult to be correlated with experiments. Hence the need of simple and graphical models that user can change and modify with minimum efforts to model their transmission systems.

3.2 Optical Fiber Impairments

1. Chromatic dispersion effects

Chromatic dispersion is a property of optical fibers which limits the performance of the communication system. It causes pulse spreading or broadening and can reduce the integrity of a received signal until appropriate dispersion compensation modules or fibers (DCM / DCF) are included in the system design.

There are two types of chromatic dispersions;

- Material Dispersion
- Waveguide Dispersion

Material dispersion arises from the change in the material's refractive index with wavelength whereas the waveguide dispersion arises from the distribution and guiding of modulated light waves between core and cladding layers. Waveguide properties are a function of the wavelength.

2. Self phase modulation (SPM)

3. Polarization mode dispersion (PMD)

The polarization mode dispersion (PMD) introduces system power penalty. It reduces the integrity of two transmitted adjacent pulses by introducing a third unwanted pulse.

4. Chirp factor

Chirp factor is responsible for the spectral broadening of the transmitted data. It also limits transmission to short distances (for $\alpha > 0$).

5. Non-linear effects

6. Receiver noise effects

The propagation models presented in this part of the report includes the SMF-28 (single mode fiber) and DCF (dispersion compensating fiber) models. Only the linear fiber model is presented whereas the non-linear model is left for future research. These models are then integrated in between the transmitter and receiver models. At the end, eye diagrams in electrical domain are used to evaluate the BER and hence the performance of the transmission system.

3.3 Corning Single Mode Optical Fiber

3.3.1 The Standard for Performance

Corning SMF-28 single mode optical fiber has set the standard for value and performance for telephony, cable television, submarine and utility network applications. Widely used in the transmission of voice, data, and video services. SMF-28 is manufactured to the most demanding specifications in the industry. SMF-28 fiber meets or exceeds ITU-T recommendation G.652.

Taking advantage of today's high capacity, low cost transmission components developed for 1550 nm window, SMF-28 fiber features low dispersion and is optimized for use in 1550 nm wavelength region.

3.3.2 Features and Benefits

- Versatility in 1310 nm and 1550 nm application
- Enhanced optical properties that optimize transmission performance
- Outstanding geometrical properties for low loss and high yield
- OVD (outside vapour deposition) manufacturing reliability and product consistency
- Optimized for use in loose tube, ribbon and other common cable designs

3.3.3 The Sales Leader

Corning SMF-28 fiber is the world's best selling fiber. In 2001, SMF-28 was deployed in over 45 countries around the world.

3.3.4 Attenuation Levels

Wavelength (nm)	Attenuation (dB/km)
1310	≤ 0.35
1550	≤ 0.22

Table 3.1

3.3.5 Dispersion

The below given formula is used to calculate the dispersion and hence employed in the calculations.

$$Dispersion = D(\lambda) \approx \frac{S_o}{4} \left[\lambda - \frac{\lambda_o^4}{\lambda^3} \right] ps / (nm.km)$$

$$1200nm \leq \lambda \leq 1600nm$$

$\lambda \rightarrow$ Operating Wavelength

where λ_o is the zero dispersion wavelength and S_o is the zero dispersion slope.

There value ranges as;

$$1302nm \leq \lambda_o \leq 1322nm$$

$$S_o \leq 0.092 ps / nm^2 .km$$

The graph given below shows the spectral attenuation of SMF-28 at different wavelengths. The value used in this report model is for 1550nm wavelength which is 0.19dB/km or 0.2dB/km.

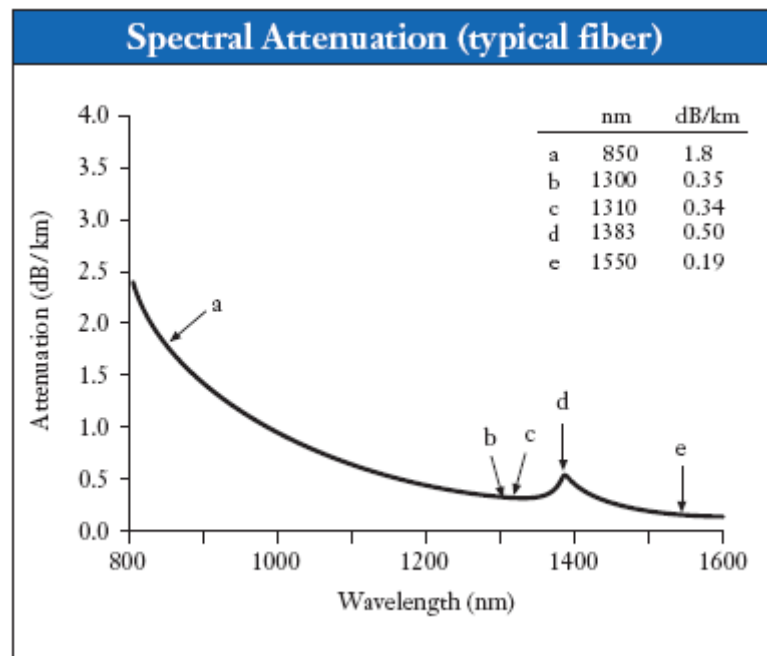


Figure 3.1 Spectral Attenuation Graph for SMF-28

3.4 Linear Fiber Propagation Model

In this report, only the linear model of light waves propagation in fiber is considered. Optical fiber allows digital light signals to propagate through long distances without the loss of signal integrity. Optical amplifiers or compensating fibers are used to compensate losses in the fiber. Fiber technology has improved dramatically with attenuation levels reaching 0.25dB/km or better in the 1550 nm C, L and S-bands.

There are several fiber models which have been proposed. One of the examples is “Fiber split step model”. The model developed in this report achieves this propagation accuracy by implementing fiber dispersion effects using time-domain digital signal processing and filtering technique that has been proven to be efficient in its computational resources. This propagation model considers the effect of dispersion directly on the system performance.

Dispersion management in high capacity (>10Gb/s) optical networks is of great importance. The fiber model includes the effects of dispersion predominantly and later analyzes the effects of different dispersion management techniques by inserting dispersion compensation fibers of varying dispersion factors (ps/nm.km). The effects of fiber attenuation considered in the model are based on standard attenuation levels of modern day single mode optical fibers (**Corning SMF-28**). This fiber model assumes that the SMF can be represented as a bandpass filter.

3.4.1 Derivation of SMF Transfer Function Model

From the time shifting property of the Fourier transform;

$$x(t_c) \leftrightarrow X(f_c)$$

$$x(t_c - \Delta t) \rightarrow e^{-j\Delta T\omega} X(f_c)$$

$$x(t_c - \Delta t) \rightarrow F[x(t_c - \Delta t)]$$

$$x(t_c - \Delta t) \rightarrow e^{-j\Delta T(2\pi f_c)} X(f_c)$$

$$x(t_c - \Delta t) \rightarrow e^{-j2\pi\Delta T f_c} X(f_c)$$

where $\Delta T = \frac{\Delta\phi}{\Delta\omega}$ is the change of phase with respect to the frequency variation.

The group velocity is dependent on the propagation constant β which is dependent on the respective refractive index for the wavelength of concern. The group velocity is also dependent on frequency of the light waves.

$$V_g \propto \frac{1}{\Delta\beta} \rightarrow V_g \propto \Delta\omega$$

$$V_g = \frac{\Delta\omega}{\Delta\beta} \rightarrow \frac{1}{V_g} = \frac{\partial\beta}{\partial\omega}$$

$$\Delta T = \frac{\partial T}{\partial\omega} = \frac{\text{distance}}{V_g} \Delta\omega$$

$$\Delta T = L \frac{\partial^2 \beta}{\partial\omega^2} \Delta\omega$$

$$T = \frac{\text{Distance}}{\text{Velocity}}$$

$$\Delta T = L \frac{D\lambda^2}{2\pi c} 2\pi\Delta f$$

$$\Delta T = \frac{LD\lambda^2}{c} \Delta f$$

$$\Delta T = \frac{LD\lambda}{f} \Delta f$$

$$\therefore X(t_c - \Delta T) \leftrightarrow X(f_c) = e^{-j\Delta T(2\pi)(f-f_c)}$$

$$e^{\frac{-j2\pi LD\lambda}{f_c}(f-f_c)^2}$$

$$e^{-j\alpha f^2}$$

The SMF transfer function linear model can thus be expressed as;

$$H(f) = e^{-j\phi(f)} = e^{-j\alpha f^2} = e^{-j \left[\alpha \beta^2 \left(\frac{f}{\beta} \right)^2 \right]}$$

$$\text{Where } \alpha = \pi D(\lambda) \frac{\lambda^2}{c} L$$

where $L=80\text{km}$, $\lambda=1550\text{nm}$, $c=3 \times 10^8 \text{ m/s}$, $f = 1.93 \times 10^{14} \text{ Hz}$, Dispersion (SMF):

$D=17\text{ps/nm.km}$ and Dispersion (DCF): $D=3\text{ps/nm.km}$

$$\begin{aligned} \therefore e^{-j\alpha f^2} &= e^{-j\pi D \frac{\lambda^2}{c} L f^2} \\ &\rightarrow e^{-j\pi D \frac{\lambda^2}{f\lambda} L f^2} \\ &\rightarrow e^{-j\pi D \lambda L f} \end{aligned}$$

where D is the dispersion, λ is the operating wavelength, L is the length of the fiber and f is the frequency of the optical carrier and its sidebands. The SMF transfer function Non Linear model can be approximated as;

$$H(f) = e^{-j\phi_{NL}}$$

$$\phi_{NL} = \gamma P_{in} L_{eff}$$

where L_{eff} is the effective length of the fiber. To remain in a linear region of fiber propagation and minimizing the effects of SPM it is recommended that $\phi_{NL} \ll 1$.

In addition to the fiber model developed, an additional non-linear phase can be added in the case where $\phi_{NL} > 0.1$. A test of the value of ' ϕ_{NL} ', which is dependant on the input power P_{in} can be performed and added into the model based on the

results of the test. With this addition, the effects of SPM on system performance could be assessed.

$$\gamma = \frac{2\pi n_2}{\lambda A_{eff}}$$

A_{eff} is the core effective area of the fiber and is given by $2\pi r_0^2$ where r_0 is the fiber spot size. The parameter n_2 is known as the material non-linear refractive index and takes the value ' $2 \times 10^{20} m^2 / W$ '.

Considering $\phi_{NL} \ll 1$, the non-linear model can be neglected. So the equivalent model for the single mode fiber can be expressed by the transfer function:

$$H(f) = e^{-j\pi D(\lambda) \frac{\lambda^2}{C} L f^2} = e^{-j\pi D(\lambda) L c} = e^{-j\pi D(\lambda) \lambda L f}$$

3.5 SIMULINK Model

As the above equation is in the form of a frequency domain transfer function, it is more convenient to operate in the frequency domain as apposed to taking the convolution in the time domain. The output of the fiber ' $\hat{X}_{out}(f)$ ', given an input modulated signal ' $\hat{X}_{in}(f)$ ' (where the ^ symbol refers to the Fast Fourier Transform (FFT) of X_{in} and X_{out}) is found by the formula:

$$\hat{X}_{out}(f) = H(f) \cdot \hat{X}_{in}(f)$$

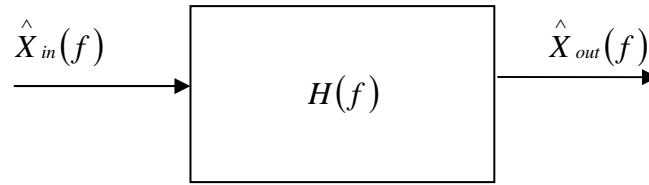


Figure 3.2 Linear Fiber Model, a Low Pass Filter

To implement the above expression, take FFT of the input modulated signal, then multiply it by $H(f)$ and take IFFT (inverse FFT) at the output. Fiber propagation model can be accurately represented with any additional chromatic dispersion, thus making the model linear.

For the standard SMF fiber model, dispersion factor is taken as $D(\lambda)_{SMF} = +17 \text{ ps/nm.km}$ at 1550 nm wavelength, $L = 80\text{km}$ with no optical amplifiers and for the dispersion compensation fiber (DCF) model smaller length is assumed where ' $D(\lambda)_{DCF} = -85 \text{ ps/nm.km}$ ', $L = 16 \text{ km}$. This value of dispersion for the DCF cancels the dispersion effects of the SMF and ensures that there is no or little loss of signal phase integrity at the receiver end. Given the Corning fiber SMF-28 manufacturers specifications quote, attenuation level of SMF-28 at 1550nm wavelength is 0.2dB/km; this implies a total of 16dB attenuation of optical power for a distance of 80km. This results in a power attenuation of 0.025 which is represented by a gain block in SIMULINK.

DCF model is also identically the same with modifications to the parameter values made as desired for dispersion compensation. It is possible to change the fiber parameters in the model directly which makes the alteration easier. The fiber model is considered to be adequate for the needs of propagation modeling along with the effects of dispersion. It is suggested that the non-linear effects be considered for future work where effects such as self phase modulation (SPM) need to be considered.

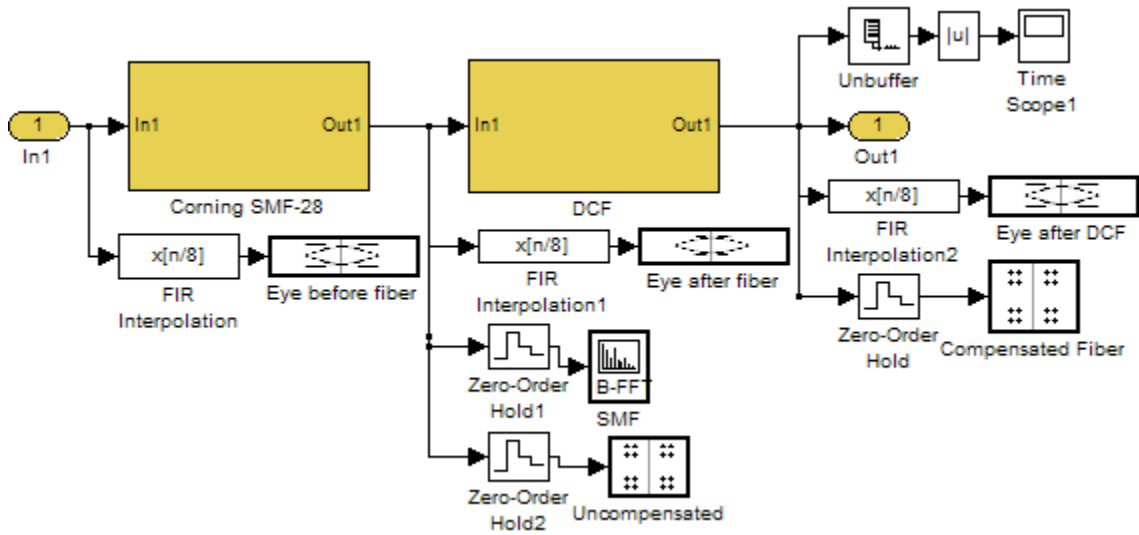


Figure 3.3 Optical Fiber Channel SIMULINK Block Model

3.6 Simulation Results

In order to retrieve the transmitted data as it was sent, all the fiber impairments and the receiver noise effects have to be compensated. Below given figures are the generated eye diagram which shows the performance of the fiber and the compensating models. Figure 3.4 shows the eye before fiber. If the same eye pattern recovers at the fiber output, that guarantees the integrity of the transmitted data otherwise not.

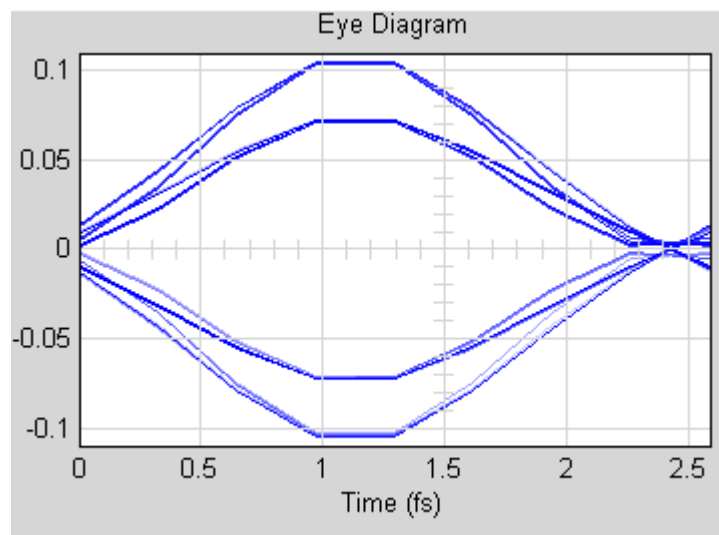


Figure 3.4 Eye Pattern before Fiber Transmission

Figure 3.5 shows the importance of the compensating fiber. When the DCF model is not inserted in the fiber model, it clearly shows the degradation in the form of the eye closure. The magnitude of the eye has been lowered significantly. Figure 3.6 shows the compensated eye which resembles the one transmitted. So how important is the dispersion compensating fiber is shown through this eye diagram.

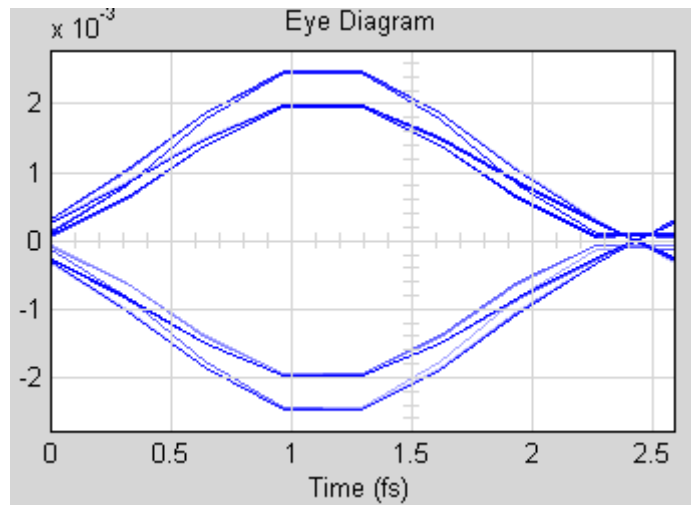


Figure 3.5 Eye Pattern after Fiber Transmission (Uncompensated)

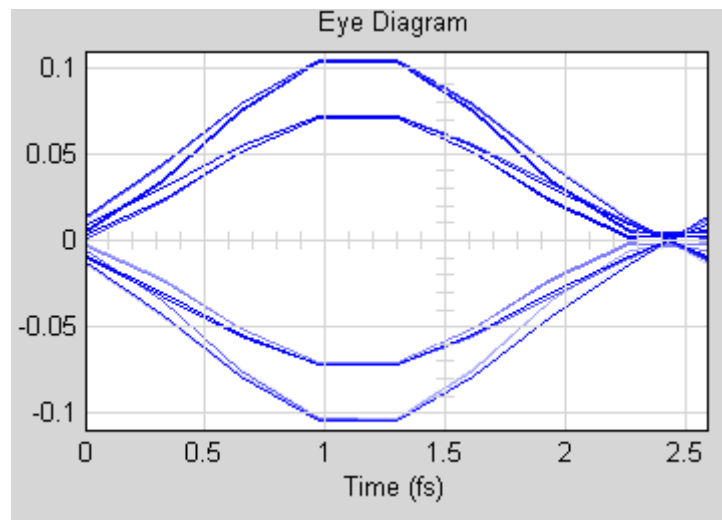


Figure 3.6 Eye Pattern after Compensation (DCF)

CHAPTER 4

RECEIVER

4.1 Receiver

In this section, the operation and theory of the optical components that are integral for the demodulation and detection of the DQPSK transmitted signal are considered. The principle operation of the receiver is to convert phase-coded information generated by the DQPSK transmitter into an intensity signal which can be detected by a photodiode circuitry at the output of the Mach-Zehnder delay interferometer (DI) arms. The intensity of the signal at the output of the DI arms is dependant on the phase difference between adjacent bits, $\Delta\phi_{\text{mod}}$ of the optical carrier in both the upper and lower arms. The relationship between phase and intensity is expressed as:

$$I(\Delta\phi_{\text{mod}}) = 0.5 \cos(\Delta\phi_{\text{mod}} \pm \frac{\pi}{4} + \delta\phi_{DI}) + 0.5$$

where ' $\delta\phi_{DI}$ ' is a phase offset. Note that this is a Mach-Zehnder device and thus operates on the principles of interference between the two arms which is dependent on the phase difference.

For the applications of DQPSK demodulation, the delay T is one bit in length (100ps for 10Gb/s operation) to allow for proper interference between two adjacent bits. Effectively the delayed signal acts as a phase reference for the incoming symbol. The extra phase delay (Phase = $\pm \frac{\pi}{4}$) is normally implemented in practice for DQPSK systems using integrated thermal heaters.

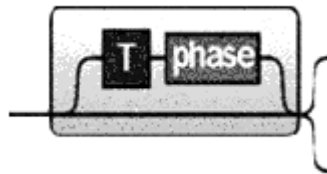


Figure 4.1 Delay Interferometer

The phase to intensity characteristic of the MZDI is shown in figure along with the expected eye diagram that allows for performance measurements to be made

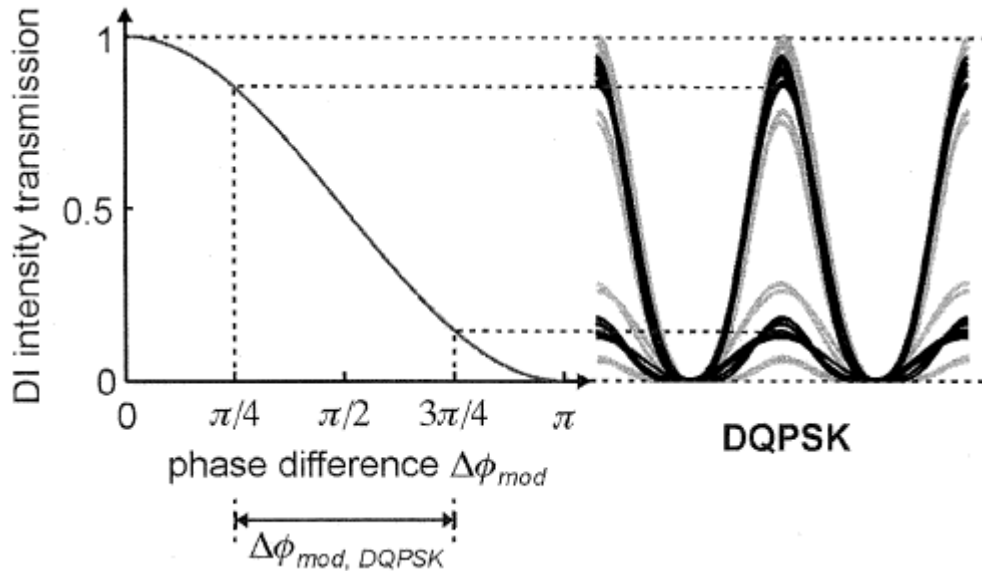


Figure 4.2 Phase to Intensity Characteristics of MZDI & The Expected Eye Diagram

The above diagram shows the Phase to Intensity characteristics of MZDI and the expected Eye Diagram generated at the output of the MZDI based on the phase difference between the two arms, lighter eye pattern is due to phase offset from heater. This optical eye diagram is then detected by a photodetector. These optical devices have shown to operate in a stable manner using either fiber-based or planar-lightwave circuit (PLC) silica on silicon technologies. The current waveform shape at the output of the photodiode has been approximated by the cos-like pulse variable in our simulations.

In order to detect the optical intensity signal at the output of the MZDI and to display this signal for later Bit Error Rate (BER) analysis, a photodiode or a pair of balanced photodiodes are required. Two types of photodiodes most commonly used in practice are PIN and the avalanche photodiode. The primary objective of the photodiode is to convert optical photonic energy to electrical current. In this

report project PIN photodiode is considered. In practice these PIN diodes (reversed-biased) are placed at the output arms of the MZDI. It's a common practice to use either single or balanced diode detection at the receiver however the balanced receiver configuration has shown higher sensitivity of 3dB improvement for DQPSK and other PSK modulation formats. In this report, a single diode detection model is developed.

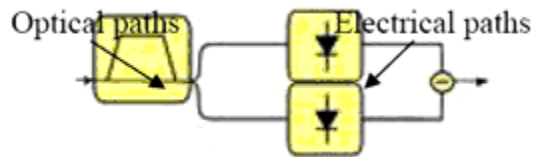


Figure 4.3 Balanced Photodiode Detection

When a modulated signal of optical power $P(t)$ falls on the detector, the primary photocurrent generated is given by:

$$I_{sig} = \eta q P \frac{\eta q P}{hf} = \mathfrak{R} P$$

where 'R' is the responsivity of the photodiode. A typical value of responsivity is 0.5 A/W.

4.2 Noise sources

In order to best simulate a true optical transmission systems, noise factors within the link are considered at the receiver end. The noise sources implemented through simulations include: the MZDI phase offset ' $\delta\phi_{DI}$ ', the photodiode noise effects (i.e. quantum shot noise, dark current and thermal noise) and the receiver amplifier equivalent noise at its input.

4.3 SIMULINK Model

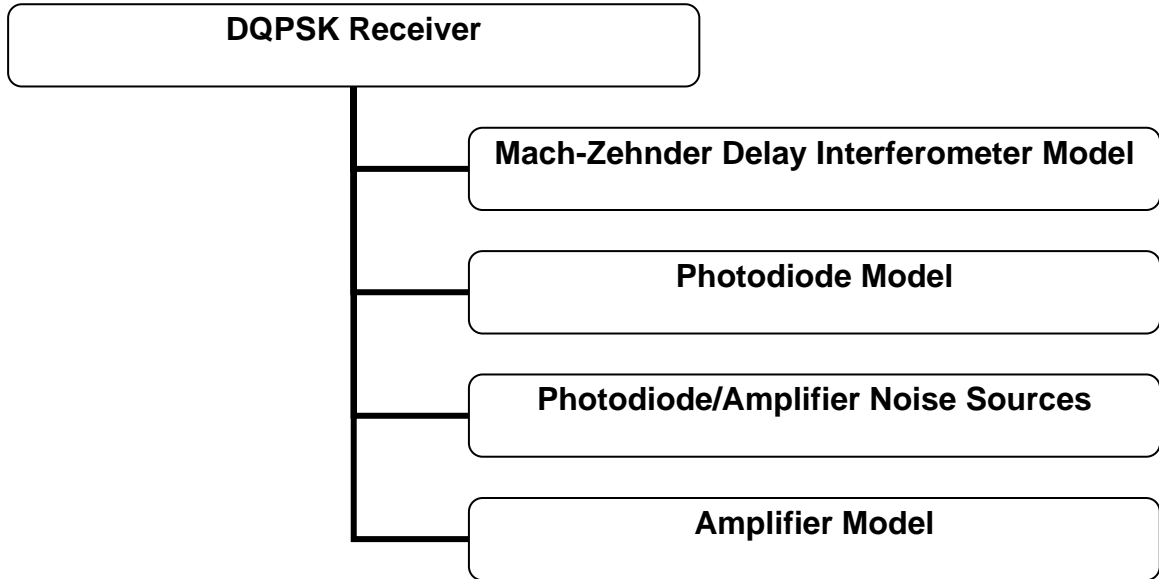


Figure 4.4 Flow Chart showing Receiver Configuration

Based on the physical setup used in practice, this model of the DQPSK receiver attempts to simulate, to within SIMULINK capabilities, some of the key principles allowing for the successful decoding of the DQPSK modulated signal. An exact receiver model is also placed before fiber to best compare the pre and post fiber effects in the form of an eye diagram. Due to the differential nature of the modulation process, the demodulation/detection stage is considered as a ‘Non Coherent’ or ‘Direct Detection’ scheme. The receiver configuration used in this report is capable of demodulating the signal transmitted along the 96 km dispersion compensated fiber span. As the modulation format used typically encodes two bits of data per symbol, it is necessary to extract both bits termed as ‘real’ and ‘imaginary’ bits from the received symbol. The receiver configuration is shown below.

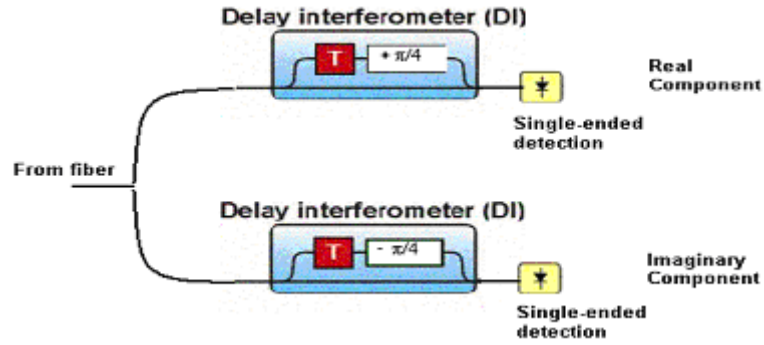


Figure 4.5 Non-Coherent Direct Detection Configuration

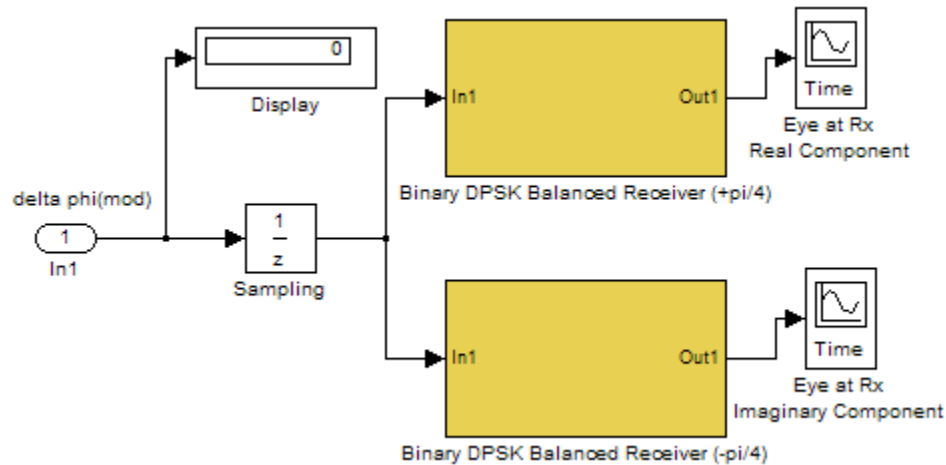


Figure 4.6 Balanced DQPSK Receiver Model

In balanced receiver configuration, there is an additional phase shift of $\pm \frac{\pi}{4}$ in the optical carrier implemented in the MZDI. Since the two bits to be encoded at the transmitter are implemented via a Phase Modulator (0 or π phase shift) and the second bit is encoded via the Phase Modulator (0 or $\frac{\pi}{2}$ phase shift), the two devices are said to be in “Quadrature” to one another. This implies that there is a $\frac{\pi}{2}$ phase difference between all signaling phase states. The additional $+\frac{\pi}{4}$ and $-\frac{\pi}{4}$ give a total $\frac{\pi}{2}$ phase difference between the upper and lower receiver

branches. In this configuration, the real and imaginary bit received can be easily compared with the one transmitted. However in this report, only the 'real component' of the received signal is considered and assessed. The overall performance of the system is measured with the help of an eye diagram (using Q-factor method and BER).

A balanced detection set up has proven to be more sensitive and 3 dB improved as compared to one photodiode detection scheme. Single photodiode detection is implemented in this report.

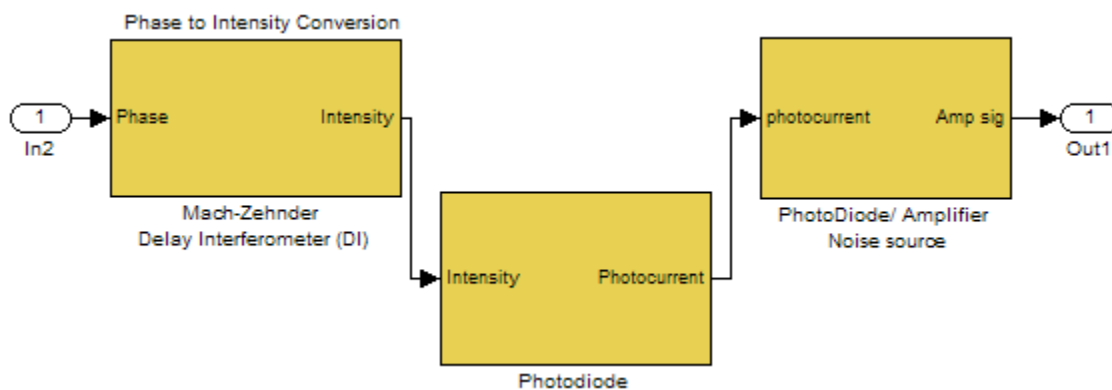


Figure 4.7 SIMULINK Block Diagram of DQPSK Receiver

4.3.1 Mach-Zehnder Delay Interferometer Model

At the input of Receiver model, there is a 'Complex Phase Difference' block. The purpose of this block is to deduce the overall phase difference between the received symbol that has been phase encoded and the reference signal given by the state of the optical carrier prior to modulation directed from the transmitter. The output of this block is constantly varying due to the periodic nature of the optical carrier; however the problem was eliminated by sampling this 'Phase difference' value every 100ps for 10Gb/s operation. The reason behind this operation is to extract the optical phase difference between adjacent symbols to perform phase to intensity conversion operation of the MZDI. This MZDI is a device to convert phase coded information into detectable intensity information.

To separate the real and the imaginary components of the received signal ' $\Delta\phi_{\text{mod}}$ ', the signal is divided into two branch configuration. $+\frac{\pi}{4}$ is added to the upper branch signal and $-\frac{\pi}{4}$ to the lower branch. Considering the real component only, when a DI phase of $+\frac{\pi}{4}$ is added to the four possible phase states of the DQPSK signaling format $\left(0, \frac{\pi}{2}, \pi, \frac{3\pi}{2}\right)$, the overall phase difference takes 'equivalent' values of $\frac{\pi}{4}$ & $\frac{3\pi}{4}$. From the values of phase obtained, it is determined that the corresponding output intensity of the MZDI by its characteristic be expressed as:

$$I = 0.5 \cos(\Delta\phi_{\text{mod}} + \Delta\phi_{\text{DI}} + \delta\phi_{\text{DI}}) + 0.5$$

$$\Delta\phi_{\text{DI}} = +\frac{\pi}{4}$$

The final term ' $\delta\phi_{\text{DI}}$ ', is referred to as the phase offset. The below given figure is the SIMULINK block diagram of MZIM showing its major components.

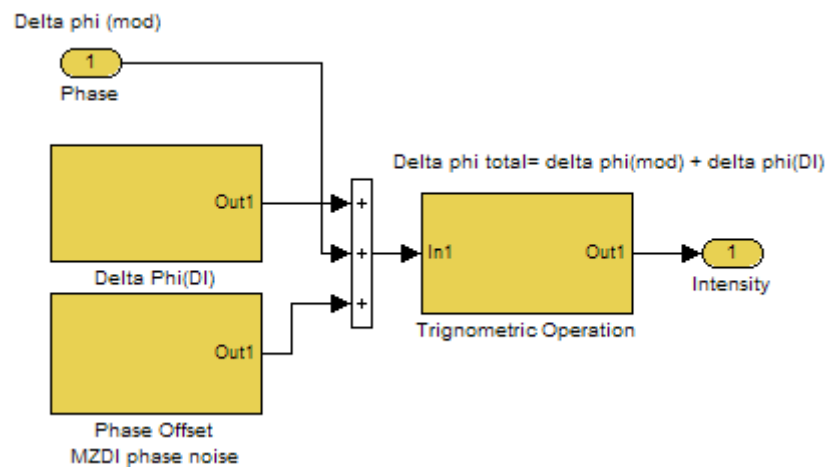


Figure 4.8 Mach-Zehnder Delay Interferometer Model

This additional phase originates from MZDI and adds extra phase noise to the system. This effect is shown to reduce eye opening and hence degrades system performance. In practice, it results due to the instability of the heaters which induce the required $+\frac{\pi}{4}$ phase shift, thus producing random values about this bias value. It is modeled in SIMULINK by assuming a maximum possible value of ' $\delta\phi_{DI}$ '. A random '*Gaussian White noise generator*' with small variance is used to represent this phase offset noise. The effects of this offset are described earlier in the eye diagram. The whole MZIM is implemented by modeling its characteristic equation already discussed above.

4.3.2 Photodiode Model

The signal after passing through MZDI enters into the Photodiode model. MZDI performed the phase to intensity conversion. Now this intensity has to be converted from optical to electrical domain which is performed by a photodiode circuitry. The photodiode modeled in this report is single ended. The intensity signal coming from MZDI is multiplied by the photodiode Responsivity ' \mathfrak{R} '. A photodiode datasheet from Discovery Semiconductor Industries is selected with a Responsivity value of 0.5A/W. The photodiode model selected is *DSC10H PIN*. Evaluating the average photocurrent given a signal of power P from the MZDI, one value is obtained between 0 and 1 as normalized current is assumed.

As the eye diagram generated by the received 'real' bits is to be analyzed, it is approximated by $Signal_{Cosine}$ variable in the simulations. MZDI characteristic is cosine shaped; it is assumed that the current waveforms forming the eye-diagram are also cosine shaped. The $Signal_{Cosine}$ variable is expressed as:

$$Signal_{Cosine} = -0.5 \cos(t) + 0.5$$

$$0 \leq t \leq 2\pi$$

The value of current is then multiplied by this variable. Finally, to complete the practical nature of the simulations, add photodiode and amplifier noise. These noise sources are superimposed on the current waveforms.

4.3.3 Photodiode/ Amplifier Noise Model

The detection of transmitted light waves is performed primarily by the photodetector. In most instances, the received optical signal is quite weak and thus electronic amplification circuitry is used, following the photodiode to ensure that an optimized power signal-to-noise ratio (SNR) is achieved. This power signal to noise ratio is calculated as follows:

$$\frac{S}{N} = \frac{I_{sig}^2}{\langle I_{noise}^2 \rangle}$$

Here I_{sig} denotes photocurrent and $\langle I_{noise}^2 \rangle$ denotes the mean squared noise contributions from the photodetector. One of the primary objectives of the noise sources is to best model optical components used in real experimental conditions. In particular the PIN photodiode and receiver total noise are calculated and superimposed over the ideal photodiode signal current. Three sources of noise include: the quantum shot noise ' i_{sh} ', the dark current noise ' i_{dk} ' and the thermal (Johnson) noise ' i_{th} '. The total current generated by the photodiode when optical power falls on it is expressed by:

$$i_{total} = i_{sig} + \sqrt{\langle i_{noise}^2 \rangle}$$

$$\langle i_{noise}^2 \rangle = \langle i_{sh}^2 \rangle + \langle i_{th}^2 \rangle + \langle i_{dk}^2 \rangle$$

It has been demonstrated that both the shot noise and dark current noise contributions from the bulk material of the photodiode follow a Poisson process, and is thus random. As a result, the mean squared values of these noise sources

are considered for calculations. The noise sources are expressed mathematically as:

$$\langle i_{sh}^2 \rangle = 2qI_{sig} B$$

$$\langle i_{dk}^2 \rangle = 2qI_{dk} B$$

Where i_{dk} is assumed to be the average dark current obtained from the semiconductor.Inc DSC10H PIN photodiode datasheet (25nA), B is the photodiode 3dB bandwidth, K_B is the Boltzmann's constant, T is the absolute temperature in Kelvin and R is the photodiode load resistor assumed to be 50ohms. The total normalized mean squared noise of $\langle i_{noise}^2 \rangle = 4.44 \times 10^{-4}$ is determined.

4.3.4 Amplifier Model

The need for amplification of the photodiode current is critical to ensure correct retrieval of data. For this purpose a gain related to an amplifier is implemented.

The amplifier is selected from MITEQ manufacturer product list with a noise figure (NF) of 0.5dB which translates to an 11% (of max current = 19.11 normalized) amplifier noise addition to the current waveform. This amplifier also has a 33dB gain which translates to a power gain of 44.67.

The addition of the photodiode noise to the photocurrent, the amplifier gain and addition of amplifier noise models developed in SIMULINK are shown in figure given below. The values of noise calculated above are maxima and are assumed to have a Gaussian distribution.

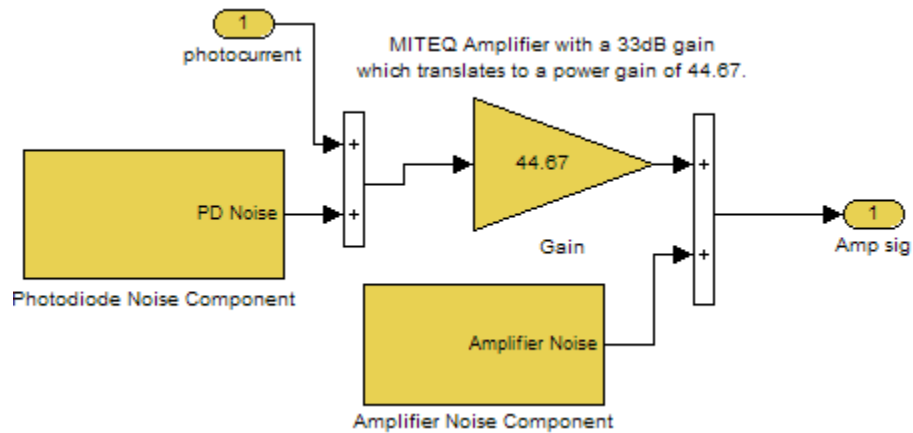


Figure 4.9 Photodiode/Amplifier Noise & Amplifier Model

		100 Davids Drive • Hauppauge • NY 11788 631-436-7400 • Fax: 631-436-7430							
MODEL NUMBER	OPERATING FREQUENCY (GHz)	GAIN (dB, Min.)	GAIN FLATNESS (±dB, Max.)	NOISE FIGURE (dB, Max.)	OUTPUT POWER (dBm, Min.)	VSWR IN/OUT (Max.)	DC POWER @ +15 V (mA)	OUTLINE DRAWING	
AMF-3F-C0200040-12-10P	0.2-0.4	48	1.5	1.2	10	2:1	200	132513	
AMF-4F-C0200040-12-10P	0.2-0.4	63	1.5	1.2	10	2:1	250	132513	
AMF-1F-C0200040-20-10P	0.2-0.4	17	1.5	2	10	2:1	100	132513	
AMF-2F-C0200040-20-10P	0.2-0.4	33	1.5	2	10	2:1	150	132513	
AMF-3F-C0200040-20-10P	0.2-0.4	48	1.5	2	10	2:1	200	132513	
AMF-4F-C0200040-20-10P	0.2-0.4	63	1.5	2	10	2:1	250	132513	
Top of page									
AMF-1F-C0250050-05-10P	0.25-0.5	17	1.5	0.5	10	2.3:1	100	132513	
AMF-2F-C0250050-05-10P	0.25-0.5	33	1	0.5	10	2:1	200	132513	
AMF-3F-C0250050-05-10P	0.25-0.5	48	1	0.5	10	2:1	200	132513	

Table 4.1 MITEQ LNA Amplifier Data Sheet

4.4 Bit Error Rate (BER) Calculations

In telecommunication, an error ratio is the ratio of the number of bits, elements, characters, or blocks incorrectly received to the total number of bits, elements, characters, or blocks sent during a specified time interval. The most commonly encountered ratio is the bit error ratio or also known as the bit error rate.

To check the reliability of any developed system, its performance has to be evaluated. The method used in this report to evaluate the system performance is the Q-factor method. Q-factor means Quality factor. It is comparatively easier to implement when the eye patterns are used.

The Q-factor is defined mathematically as;

$$Q = \frac{\mu_1 - \mu_0}{\sigma'_1 + \sigma'_0}$$

Where the numerator calculates the magnitude difference between the upper and the lower eye lobe and the denominator calculates the noise jitter. The typical values of these noise jitters for Gaussian pulses are;

$$\sigma'_0 = 0.68\sigma_0$$

$$\sigma'_1 = 0.68\sigma_1$$

The corresponding BER can be calculated by below mentioned formula.

$$BER \approx \frac{\exp(-Q^2 / 2)}{Q\sqrt{2\pi}}$$

4.5 Simulation Results

Figure 4.10 shows the received data constellation when no DCF (dispersion compensating fiber) was inserted. The data is highly corrupted and no useful information can be retrieved. The figure shows that all the four data constellation points are merged into one another. To avoid such situation DCF must be inserted to get better results.

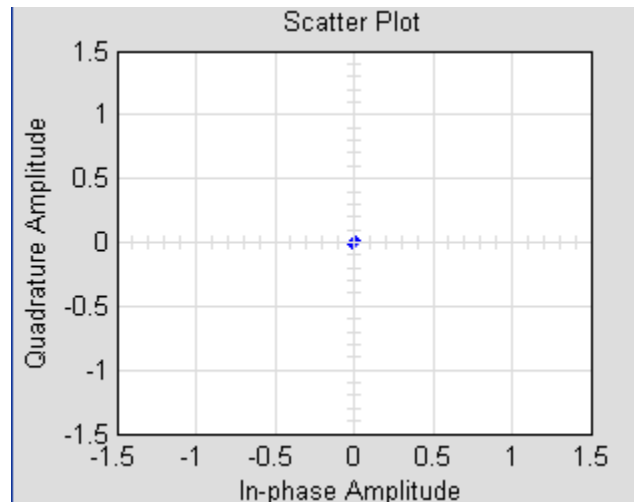


Figure 4.10 Uncompensated Received Data

Now the DCF has been inserted and a clear difference can be seen from the received data constellation. The recovered data is very much closer to the one transmitted hence the desired result. The results can further be improved by using more negative values of DCF dispersion factor. In this report, the optimal dispersion factor calculated is -97ps/nm.km .

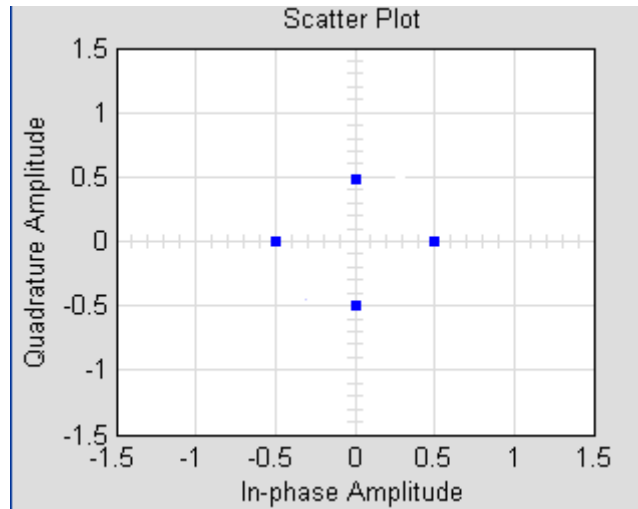


Figure 4.11 DCF Compensated Received Data

Figure 4.12 and onwards show the eye pattern comparison between the transmitted and the received data. It is very obvious that how the signal degrades when it propagates.

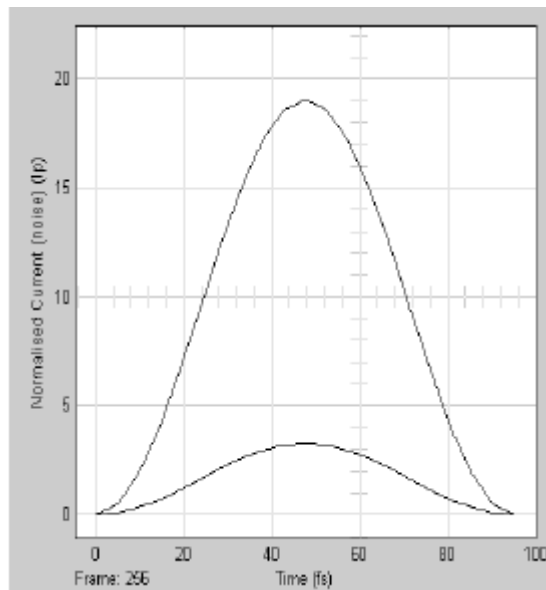
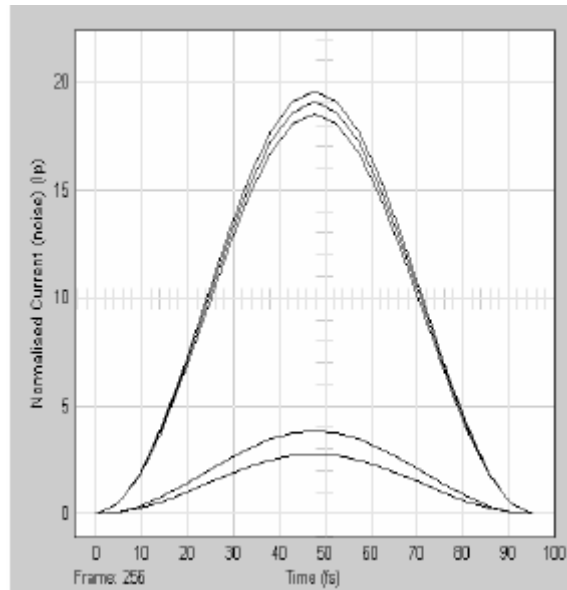


Figure 4.12 Transmitted Signal's Eye Diagram

Figure 4.13 shows the eye pattern when no DCF, photodiode and amplifier noise are added in the model. The figure shows three traces.



**Figure 4.13 Received Signal's Eye Diagram
No DCF, PD & Amplifier Noise added**

Figure 4.14 to 4.17 are the eye comparisons by changing the dispersion factors. It is observed that the noise jitter minimizes with the increase in the negative dispersion value. The model is evaluated at -65 , -75 and -95 ps/nm.km dispersion factors. The best results were found with the dispersion factor of -95 ps/nm.km. At this dispersion value, the bit error rate calculated is 1.6×10^{-8} which is comparable with the published paper experimental result. The last two eye diagrams shows this result.

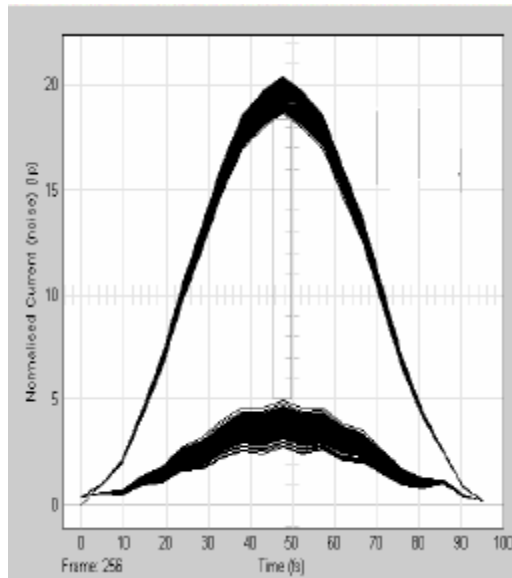


Figure 4.14 Received Signal's Eye
Dispersion= -75ps/nm.km, Q-factor = 4.62, BER = 1.9e-6

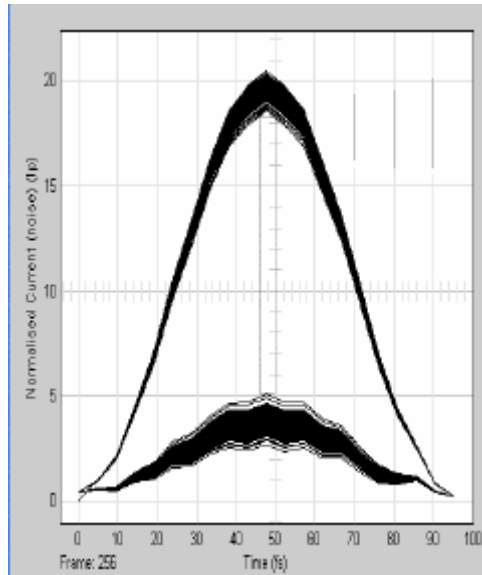


Figure 4.15 Received Signal's Eye
Dispersion= -65ps/nm.km, Q-factor = 4.28, BER = 9.3e-6

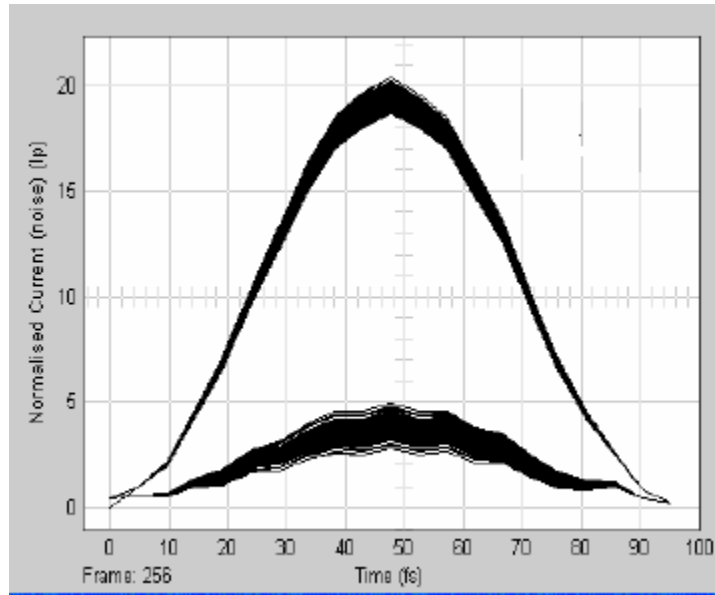


Figure 4.16 Received Signal's Eye

Dispersion= -95ps/nm.km, Q-factor = 5.3, BER = 1.0e-8

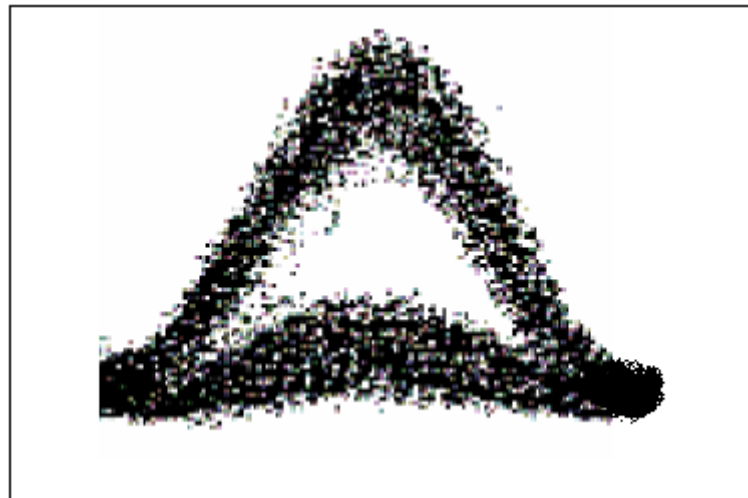


Figure 4.17 Experimental Result with BER = 1.0e-8

CHAPTER 5

CONCLUSION & RECOMMENDATIONS

5.1 Concluding Remarks & Recommendations

In this report, three main components were considered which form a single channel optical fiber communication link. The components include transmitter, optical fibers –standard and compensating types and receiver. Although, there are different proposals made to date for improved fiber transmission, even the DQPSK technique also but the two phase modulator's idea and DQPSK balanced detection scheme implemented in the same model is for the first time. The flexible nature of SIMULINK and its wide range of pre-designed block sets allow several important features for implementation of optically amplified transmission systems.

It is found that DQPSK modulation format is implemented in different ways using alternative hardware ranging from integrated lasers and dual drive Mach-Zehnder modulator devices to simple configurations using MZIMs and Phase Modulators. In this report, DQPSK modulation format proved to offer twice the bandwidth compared to conventional OOK (On-Off Keying). Apart from the Di-bit coding aspect of this modulation format and increased spectral efficiency (b/s/Hz), presentation of results proved the superiority of this format. Balanced detection scheme used in receiver significantly improved the BER performance by at least 3.5 dB. Although non-linear model was not considered in this report, however linear fiber model as a low pass filter proved to present sufficiently accurate on dispersion effects provided the total optical power is below the nonlinear SPM (self phase modulation) threshold. The simplicity to develop in SIMULINK environment was also a positive factor.

The development of the model for 10Gb/s single channel DQPSK transmission system has been proposed to provide, unlike other commercial packages such as VPI Systems, the most effective and simplified simulation package. This model has simulated the most complex modulation format of the family of optical modulation techniques proposed in literature of digital optical communications. The nature in which the model has been designed in SIMULINK allows for future

development of the DPSK (Differential phase shift keying) and other optical modulation formats, e.g. multi-level M-ary schemes. This technique has also been well explored in practice and is derived from the same differential phase coding principle as DQPSK.

To implement this system, only one phase modulator (PM) will be needed in the transmitter and one pair of MZDI at the receiver would be required for the in-phase and quadrature phase channels. In addition, the $\pi/4$ phase shift incorporated into the MZDI upper arm would be set to zero. Because only the 0 and π symbol phase states are needed, the eye diagram is expected to form a constellation and hence improvement of the receiver sensitivity, resulting in higher Q-factors and thus lower BER. Although higher sensitivity would be achieved, this technique comes at the expense of only transmitting 1 bit/symbol as opposed to 2 bits/symbol of the DQPSK system.

The dispersion management technique implemented in this report that is the dispersion compensating fiber is also used in practice. The SIMULINK model reported here considered only the transmission fiber, spanning a total length of 96 km. Multi-span long-haul dispersion managed transmission can be extended without difficulty incorporating EDFA pre-amplifier and booster amplifiers. Several spans of SMF and DCF fiber and optically amplified models can be cascaded.

The combinations of SMF and DCF would, in practice need to be compensated by optical amplifiers (~every 80 to 100 km). EDFAs or Raman Optical Amplifiers have been currently developed and can also be included in this SIMULINK model for better results. This simulation system can be extended and used as a useful tool for assessing designs of Super DWDM optical fiber networks implementing in particular, DQPSK systems, thus allowing transmission capacities to be simulated to the Terabits/sec capacity.

The optical components modeled in this report are all commercially available; hence the model can be easily implemented in practice. Furthermore considering the recent increasing demands of data bandwidth, system designs such as DWDM, with increased channel capacity using existing available photonic hardware are of significant importance.

Apart from system configuration, modulation formats used to transmit data can also increase data transmission capacity with its effective bandwidth. It is thus possible to remove the limitations of hardware and use signaling aspects to improve transmission capacity. This report model demonstrated a 20Gb/s (2x10Gb/s) single channel optical DQPSK model which is capable of doubling the bit rate compared to conventional OOK signaling techniques. The simulator has been developed in the MATLAB subsidiary program SIMULINK. The ease with which a model can be altered made it possible to optimize the system in future.

All the optical components necessary for transmission, propagation and detection of the data have been implemented in the SIMULINK along with the added noise sources. Transmitter components include the Mach-Zehnder Interferometer component, phase modulators along with the optical carrier and electrical bit stream binary generators. The fiber has been developed using a linear Low Pass Filter model which only takes into account the linear dispersion effects of optical fibers. It has been shown that without appropriate dispersion management, the phase information coded in adjacent symbols is corrupted. SIMULINK made it easy to check the system performance by changing the parameter values without changing the whole model. This research can be extended to simulate dense and super-dense WDM long-haul transmission systems. This work has provided the framework for individual channels that would compose the DWDM system. It has been successfully demonstrated that 20Gb/s DQPSK transmission with a BER of 10⁻¹², an extension to Tb/s system would be possible.

Appendix

MATLAB m-file

Standard system parameters

```
bitrate=10*10^9 %bitrate in b/s  
bitnum=256 %number of bits in data string,  
lambda=1550e-9 %operating wavelength in m  
Ts=2.59*10^-15 %sampling time
```

Fiber Parameters (optional parameters varied for different fibers)

```
Dsmf=17e-6 %SMF dispersion factor in s/m^2  
Ddcf=-85e-6 %DCF dispersion factor in s/m^2  
Lsmf=80000 %SMF fiber length in m  
Ldcf=16000 %DCF fiber length in m  
speedlight=3*10^8 %speed of light in m/s
```

System functions

```
time=(bitnum-1)*(1/bitrate) %simulation time for desired bit string
```

Photodiode Parameters

```
R = 0.5 %Responsivity (1550nm) From DSC 10H PIN Data Sheet  
DarkI = 25 %Dark current in nA  
Pmax = 20 %Maximum power rating in mW
```

Inverted Cos-like photodiode current pulse approximation

```
t = 0:pi/10:2*pi;  
SignalCosine = -0.5*cos(t)+0.5;  
end of initialization file
```

References

- [1] B. Zhu, "3.08Tbit/s WDM transmission over 1200 km fiber with 100 km repeater spacing using dual C and L band hybrid Raman/Erbium-doped inline amplifiers", *Electronics Letter*, vol.37, 2001.
- [2] E. Yamada, "106 channel 10Gbit/s, 640km DWDM transmission with 25GHz spacing with super continuum multi-carrier source", *Electronics Letter*, vol.37, 2001.
- [3] C. Wree; "RZ-DQPSK format with high spectral efficiency and high robustness towards fiber nonlinearities"; University of Kiel, 2002.
- [4] A. Carena, "A time domain optical transmission system simulation package accounting for Nonlinear and Polarization-related effects in fiber"; *IEEE Journal*; vol.15, 1997.
- [5] J. T. Gallo, "Optical Modulators for fiber systems", presented at IEEE GaAs Digest; p.145, 2003.
- [6] A. F. Elrefaie, "Chromatic Dispersion limitations in coherent lightwave transmission systems", *IEEE Journal Lightwave Technology*, vol.6, 1988.
- [7] "Corning :Fiber-Optic Technology Tutorial"; *The International Engineering Consortium*.
- [8] S. V. Kartalopoulos, "*Introduction to DWDM technology: Data in a rainbow*"; J Wiley, 2001.
- [9] K. P. Ho, "Raised Cosine function in time domain as defined "Spectrum of externally modulated optical signals", *IEEE Journal Lightwave Technology*, 2004.

- [10] H. Kim, "Robustness to Laser Frequency Offset in Direct-Detection DPSK and DQPSK systems", *IEEE Journal Lightwave Technology*, vol.21, 2000.
- [11] A. W. Gnauck A.H., P.J., "Tutorial on Phase-Shift-Keyed Transmission", presented at OFC 2004, 2004.
- [12] S. E. Miller, "*Optical Fiber Communication 2*"; Academic Press, 1988.
- [13] C. Wree, "Experimental Investigation of receiver sensitivity of RZ-DQPSK modulation format using balanced detection", presented at OFC 2003, 2003.
- [14] P. E. Green, "*Fiber Optic Networks*": Prentice Hall, 1993.
- [15] J. G. Proakis, "*Digital Communications*", 3rd edition, McGraw-Hill, 1995.
- [16] J. C. Palais, "*Fiber Optic Communications*": Prentice Hall, 1984.
- [17] G. P. Agrawal "*Fiber-optic Communication Systems*", 2nd ed. N.Y, Academic Press, 2002.
- [18] G. Keiser, "*Optical Fiber Communication*", New York: McGraw Hill, 1991.
- [19] X. Wei, "Numerical Simulation of the SPM penalty in a 10Gb/s RZ-DPSK system" *IEEE Photonics technology Letters*, vol. 15, 2003.
- [20] [http// www.wikipedia.org](http://www.wikipedia.org)
- [21] [http// www.google.com](http://www.google.com)